碩士學位論文

Synthesis and Characterization of Dinuclear Cobalt(II or III)-N_4O_2 Compartmental Macrocyclic Complexes Containing Auxiliary Ligands with 2,6-Diformyl-*p*-cresol and *trans*-1,2-Diaminocyclohexane

Supervised by professor Jong-Chul Byun

Major in Chemistry Education
Graduate School of Education
Cheju National University

Chang-Sik Hyun

August, 2005

碩士學位論文

2,6-diformyl-*p*-cresol과 *trans*-1,2-diaminocyclohexane에 의한 N_4O_2 칸막이형 거대고리-cobalt(II or III) 착물과 보조 리간드간의 화합물 합성 및 특성

指導敎授　卞　鍾　轍

濟州大學校 敎育大學院

化學敎育專攻

玄　昌　埴

2005年　8月

2,6-diformyl-*p*-cresol과 *trans*-1,2-diaminocyclohexane에 의한 N_4O_2 칸막이형 거대고리-cobalt(II or III) 착물과 보조 리간드간의 화합물 합성 및 특성

指導敎授 卞 鍾 轍

이 論文을 敎育學碩士學位論文으로 提出함.

2005년 8월

濟州大學校 敎育大學院 化學敎育專攻

玄 昌 埴

玄 昌 埴의 敎育學 碩士學位 論文을 認准함.

2005년 8월

審査委員長 _____ 印

審査 委員 _____ 印

審査 委員 _____ 印

Synthesis and Characterization of Dinuclear Cobalt(II or III)-N_4O_2 Compartmental Macrocyclic Complexes Containing Auxiliary Ligands with 2,6-Diformyl-*p*-cresol and *trans*-1,2-Diaminocyclohexane

Chang-Sik Hyun
(Supervised by professor **Jong-Chul Byun**)

A thesis submitted in partial fulfillment of the requirement for the degree of Master of Education

2005. 8. .

This thesis has been examined and approved.

Date Approved :

_____

_____

_____

_____

Major in Chemistry Education
Graduated School of Education
Cheju National University

Abstract

Synthesis and Characterization of Dinuclear Cobalt(II or III)-N_4O_2 Compartmental Macrocyclic Complexes Containing Auxiliary Ligands with 2,6-Diformyl-*p*-cresol and *trans*-1,2-Diaminocyclohexane

Hyun, Chang-Sik

Chemistry Education Major
Graduate School of Education, Cheju National University
Cheju, Korea

Supervised by Professor Byun, Jong-Chul

The reaction of 2,6-diformyl-*p*-cresol and trans-1,2-diaminocyclohexane in methanol in equimolar ratio using the high dilution technique affords a [3 + 3] Schiff-base macrocycle L_3 as yellow solid in high yield. The CHN, IR, NMR and FAB mass spectral data of the product do not agree with the expected a [2 + 2] Schiff-base macrocycle ligand L_2 (= H_2[20]-DCHDC) but match with the composition of [3 + 3] Schiff-base macrocycle L_3.

Dinuclear Co(II) complexe, $[Co_2([20]\text{-DCHDC})Cl_2]\cdot 2H_2O$, with [2 + 2] symmetrical N_4O_2 compartmental macrocyclic ligand containing bridging phenolic oxygen atoms was synthesized by metal template condensation of 2,6-diformyl-*p*-cresol, trans-1,2-diamino-cyclohexane, and $CoCl_2 \cdot 6H_2O$. The reaction of $[Co_2([20]\text{-DCHDC})Cl_2]\cdot 2H_2O$ with auxiliary ligands (L_a; ClO_4^-, CN^-, NCS^-, NO_2^-, NO_3^-, N_3^-) in aqueous solution formed a new 6 complexes; $[Co_2([20]\text{-DCHDC})(\mu\text{-}O_2ClO_2)_2] \cdot H_2O$, $[Co_2([20]\text{-DCHDC})(CN)_2] \cdot 2H_2O$, $[Co_2([20]\text{-DCHDC})(NCS)_2] \cdot 2H_2O$, $[Co_2([20]\text{-DCHDC})(NO_2)_2] \cdot 3.5H_2O$, $[Co_2([20]\text{-DCHDC})(OH_2)_4](NO_3)_2$, $[Co_2([20]\text{-DCHDC})(N_3)_3(OH)]$. These complexes have been characterized by a combination of elemental analysis, conductivity, IR, UV-Vis and mass spectrometer .

※ A thesis submitted to the Committee of the Graduate School of Education, Cheju National University in partial fulfillment of the requirements for the degree of Master of Education in 2005, 8, .

Contents

List of Tables

List of Figures

I. Introduction

Interest in exploring metal ion complexes with macrocyclic ligands has been continually increasing owing to the recognition of their role played by these structures in metalloproteines. Schiff base macrocycles have been of great importance in macrocyclic chemistry. They were among the first artificial metal macrocyclic complexes to be synthesized. The metal complexes containing synthetic macrocyclic ligands have attracted a great deal of attention because they can be used as models for more intricate biological macrocyclic systems: metalloporphyrins (hemoglobin, myoglobin, cytochrome, chlorophyll), corrins (vitamin B_{12}) and antibiotics (valinomycin, nonactin). These discoveries have created supramolecular chemistry and its enormous diversity [1-5].

Over the past decade, many studies have been focused on the design, template synthesis and characterization of the new supramolecular polyaza and polyoxaaza Schiff base mono- and homo- or heterodinuclear macrocyclic complexes of metal ions of varying radii and electron configuration - in particular rare earth elements - and the factors which prove to be of importance in directing the synthetic pathway in these systems.

The Schiff base macrocyclic complexes, which form neutral or cationic complexes with the metal of interest, fulfill these requirements, because they are extremely rigid and display kinetic inertness towards metal release, whereas exocyclic ligands are labile and easy to change.

Macrocyclic Schiff bases have been widely studied because they can selectively chelate certain metal ions depending on the number, type and position

of their donor atoms, the ionic radius of the metal center, and coordinating properties of counter ions.

Co(II) complexes with polyamine ligands containing binding units suited for the coordination of a single metal ion or for the dinuclear centers have proved very useful. The structure of these synthetic dioxygen carriers, the kinetics and thermo-dynamics of their formation is affected by the nature of the ligand. The use of polynucleating ligands represents an evolution in synthetic Co(II) dioxygen carriers. These ligands contain sufficient number of oxygen and nitrogen donor atoms to coordinate more than one Co(II) ion and can act as biomimetic models of natural non-heme types carriers, such as hemerythrin and hemocyanin.[6]

1. Template synthesis of Schiff base macrocyclic complexes

Recognition of the importance of complexes containing macrocyclic ligands for supramolecular science, bioinorganic chemistry, biomedical applications, separation and encapsulation processes as well as formation of compounds with unusual properties and structures has led to considerable effort to develop methods for the synthesis of these compounds. The macrocyclic complex is formed by adding the required metal ion to a preformed macrocycle. However, the direct synthesis of macrocycles often results in very low yield of the desired product with the domination of competing linear polymerization or other side reactions.

Many synthetic routes to macrocyclic ligands involve the use of the metal ion template to orient the reacting groups of linear substrates in the desired conformation for the ring to close. The favorable enthalpy for the formation of metal-ligand bonds overcomes the unfavorable entropy of the ordering of the

multidentate ligand around the metal ion and hence it promotes the cyclization reaction [1, 14, 15]. The effective method for the synthesis of Schiff base macrocyclic complexes which involves the condensation reaction between suitable dicarbonyl compounds and primary diamines carried out in the presence of appropriate metal ions which serve as templates in directing the steric course of the reaction. In this metal template effect the metal ion - through coordination - organizes the linear substrates to facilitate the condensation process which may lead toward either [1 + 1] or [2 + 2] macrocyclic products.

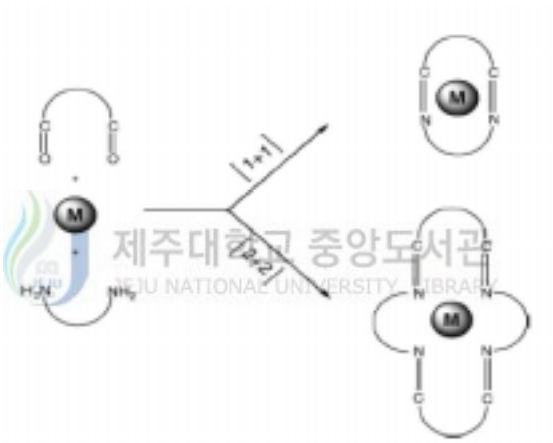

Whether the cyclization proceeds through an intramolecular condensation to give a [1 + 1] macrocycle or through the bimolecular steps leading to a [2 + 2] macrocycle depends on the relative proportions of linear substrates, the nature of the cation and reactants (chain length, number and location of potential donor atoms), the ratio of the template ionic radius to the cavity size, conformation of acyclic intermediates and coordination properties of counter ions. Rare earth metal ions have found to be very efficient metal templates in the synthesis of the complexes of this type. The first example of such an action of these ions in

the synthesis of polyaza Schiff base macrocyclic compounds was reported for scandium(III) ion [16]. Rare earth elements are known to have little or no stereochemical requirements and can be accommodated by the stereochemical constraints enforced by the template process. In some cases the mononuclear or dinuclear open-chain chelates with two terminal carbonyl groups or one terminal carbonyl group and one terminal amine group - considered as potential intermediates in the template process [1, 14, 15] - can be the final products of the Schiff base condensation [17-22]. The formation of these compounds instead of the expected macrocycles may be attributed to the unfavorable positioning of the terminal groups which decreases the probability of intermolecular linkage with next diamine molecule or a possibility of the nucleophilic attack of the amine nitrogen on the carbon atom of the carbonyl group and stabilizes the open-chain product once formed. The investigation of the mechanism of the formation of Schiff base complexes demonstrates that the structure and coordination mode of potential intermediates is one of the key factors that determine the preferred pathway of the metal-ion templated condensation in the Schiff base systems and must be taken into account in the design and synthesis of desired products.

2. Chiral Schiff base macrocycles

The introduction of chiral diamines in the synthesis of hexaazamacrocycles leads to chiral macrocyclic lanthanide(III) complexes. These compounds are interesting from the perspective of a recent application of lanthanide(III)

complexes of chiral crown ethers as enantioselective catalysts [23, 24].

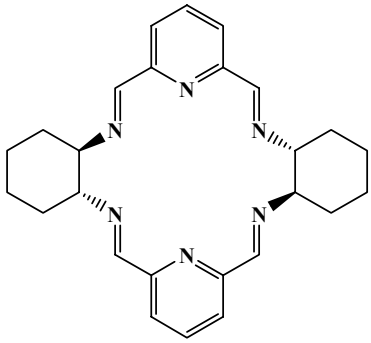

L_1

The first Schiff base complexes of this type were obtained for the ligand L_1, both as racemates [24] and in the enantiopure form [25, 26]. The latter complexes have been shown to exhibit circularly polarized luminescence and their photophysical properties have been studied in detail [26].

In this work, the dinuclear Co(Ⅱ or Ⅲ) complexes $[Co_2([20]\text{-DCHDC})(L_a)_n]^{(2-n)+}$ has been synthesized by metal template condensation of 2,6-diformyl-*p*-cresol, trans-1,2-diaminocyclohexane, and $CoCl_2 \cdot 6H_2O$. The reaction of $[Co_2([20]\text{-DCHDC})Cl_2] \cdot 2H_2O$ with auxiliary ligands (L_a; ClO_4^-, CN^-, NCS^-, NO_2^-, NO_3^-, N_3^-) in aqueous solution formed a new 6 complexes. The physical characterization of the new complexes has been explained by means of elemental analysis, FT-IR, UV-Vis spectrophotometer, conductivity and FAB-mass spectrometer.

II. Experimental section

1. Physical Measurements

All chemicals were commercial analytical reagents and were used without further purification. For the spectroscopic and physical measurements, organic solvents were dried and purified according to the literature methods [27]. Nanopure quality water was used throughout this work. Microanalyses of C, H, and N were carried out using LECO CHN-900 analyzer. NMR spectra were obtained with a JNM-LA400 FT-NMR (JEOL) Spectrophotometer. Conductance measurements of the complexes were performed at 25±1℃ using an ORION 162 conductivity temperature meter. IR spectra were recorded with a Bruker FSS66 FT-IR spectrometer in the range 4000-370 cm^{-1} using KBr pellets. Electronic absorption spectra were measured at 25℃ on a UV-3150 UV-VIS-NIR Spectrophotometer (SHIMADZU). FAB-mass spectra were obtained on a JEOL JMS-700 Mass Spectrometer using argon (6 kV, 10 mA) as the FAB gas. The accelerating voltage was 10 kV andglycerol was used as the matrix. The mass spectrometer was operated in positive ion mode and mass spectrum was calibrated by Alkali-CsI positive.

2. Synthesis of Ligand and Complexes

1) Preparation of 2, 6-diformyl-*p*-cresol.

The synthesis of 2,6-diformyl-*p*-cresol was prepared according to the methods previously reported.[28, 29]

2) Preparation of the macrocyclic ligand with 2,6-diformyl-*p*-cresol and *trans*-1,2-diaminocyclohexane.

To a solution of trans-1,2-diaminocyclohexane (0.48 mL) in 50 mL of methanol was added dropwise a hot solution of 2,6-diformyl-*p*-cresol (0.656 g) in 50 mL of methanol and the resulting red solution was refluxed for 3 h, after which time a yellow compound separated out. The solution was cooled to room temperature and the yellow product was filtered, thoroughly washed with ice-cold methanol, and dried under vacuum

Yield 0.8843 g (89%).

Anal. Calc. (%) for : $(C_{45}H_{54}N_6O_3)(H_2O)$:

C, 72.55 ; H, 7.58 ; N, 11.28.

Found (%) : C, 72.75 ; H, 7.03 ; N, 11.33.

Solubility : DMF, acetone, chloroform, THF.

UV-Vis (DMF) [λ_{max} (nm) (ε ($M^{-1}cm^{-1}$))] : 450 br (474)

λ_M (DMF) : 0.32 $ohm^{-1}cm^2mol^{-1}$.

FAB-mass : Calc. for $C_{45}H_{54}N_6O_3$ m/z 727. Found 727.4 (M^+).

^{1}H-NMR ($CDCl_3$, ppm) : 8.670 (s, HC=N), 8.210 (s, HC=N), 7.576 (s, Ar-H), 6.898 (s, Ar-H), 3.383 (m, N-CH, cyclohexane), 2.079 (s, Ar-CH_3), 1.845-1.469 (m, CH_2CH_2, cyclohexane).

^{13}C-NMR ($CDCl_3$, ppm) : 19.98, 24.40, 33.15, 33.45, 73.29, 75.36, 118.77, 122.959, 126.84, 129.62, 134.21, 156.18, 159.46, 163.46.

FT-IR (KBr, cm^{-1}) : 3439 (br), 3018, 2926, 2856, 1638(ν(C=N), 1601, 1447, 1390, 1371, 1312, 1258, 868, 827, 761.

3) Preparation of dinuclear Co(Ⅱ or Ⅲ) complexes.

The dinuclear Co(Ⅱ or Ⅲ) complexes with [2 + 2] symmetrical N_4O_2 compartmental macrocyclic ligand {([20]-DCHDC)$^{2+}$} containing bridging phenolic oxygen atoms was synthesized by condensation of 2,6-diformyl-*p*-cresol and *trans*-1,2-diaminocyclohexane, in the Co(Ⅱ or Ⅲ) ions (Scheme 1).

(1) $[Co_2([20]\text{-DCHDC})Cl_2] \cdot 2H_2O$.

Cobalt chloride hexahydrate (9.48 g), 2,6-diformyl-*p*-cresol (4.92 g), and *trans*-1,2-diaminocyclohexane (3.60 g) in methanol (150 mL) were refluxed for 1day. The solution was concentrated under vacuum to approximate 50 mL and then it was on standing overnight at room temperature. The resulting dark green precipitate was filtered, thoroughly washed twice with methanol, dried under vacuum over anhydrouse calcium chloride.

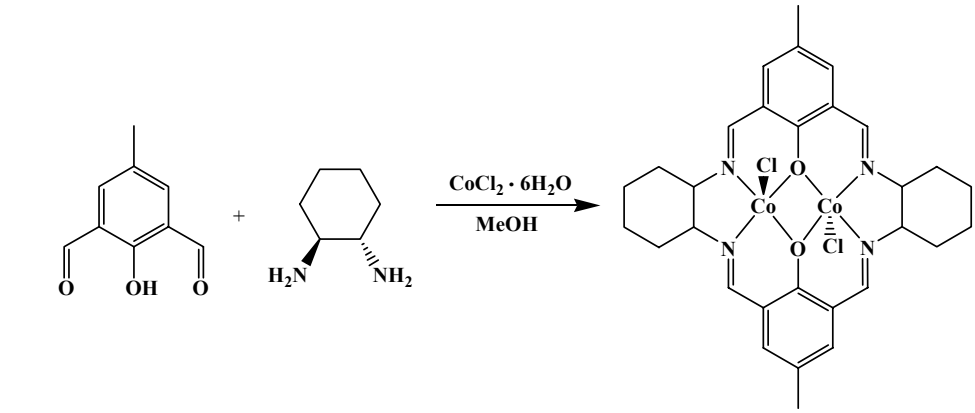

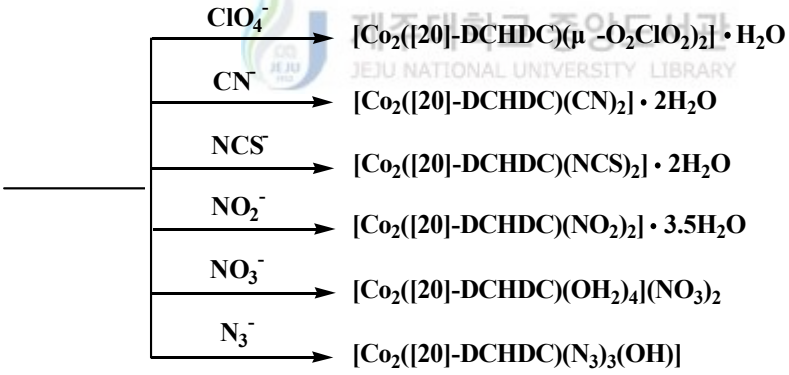

Scheme 1. Synthesis of the dinuclear Co(Ⅱ or Ⅲ) complexes of phenol-based macrocyclic ligand

Yield : 8.5842 g (80.9%)

Anal. Calc.(%) for $Co_2(C_{30}H_{34}N_4O_2)Cl_2(H_2O)_2$

C, 50.94 ; H, 5.41 ; N, 7.92

Found(%) C, 51.09 ; H, 5.26 ; N, 7.90

solubility : water, MeOH, hot Acetonitrile, hot DMSO

λ_M (DMSO) : 25 $ohm^{-1}cm^2mol^{-1}$

(2) $[Co_2([20]\text{-DCHDC})(\mu\text{-}O_2ClO_2)_2] \cdot H_2O$

A solution of $[Co_2([20]\text{-DCHDC})Cl_2] \cdot 2H_2O$ (0.707 g) in water (100 mL) was added slow dropwise a saturated aqueous sodium perchlorate solution (4 mL) with stirring and a solution was refluxed for 4 h. The resulting dark brown precipitate was filtered, thoroughly washed twice with water, and dried under vacuum.

Yield : 0.7747 g (94.7%)

Anal. Calc.(%) for $Co_2(C_{30}H_{34}N_4O_2)(ClO_4)_2(H_2O)$

C, 44.08 ; H, 4.44 ; N, 6.85

Found(%) C, 44.08 ; H, 4.71 ; N, 6.30

solubility : DMSO, DMF, hot MeOH, hot Acetonitrile, hot Acetone

λ_M (DMSO) : 49.4 $ohm^{-1}cm^2mol^{-1}$

(3) $[Co_2([20]\text{-DCHDC})(CN)_2] \cdot 2H_2O$.

A solution of $[Co_2([20]\text{-DCHDC})Cl_2] \cdot 2H_2O$(0.707 g) in hot water (100 mL)

was added dropwise a solution of sodium cyanide (0.49 g) in water (30 mL) with stirring and the mixture was reflux whereupon the initial yellow-brown precipitate first turned dark orange. The resulting dark orange precipitate was filtered, thoroughly washed twice with water, and dried under vacuum.

Yield : 0.5590 g (81.2%)

Anal. Calc.(%) for $Co_2(C_{30}H_{34}N_4O_2)(CN)_2(H_2O)_2$

C, 55.82 ; H, 5.56 ; N, 12.21

Found(%) C, 55.48 ; H, 5.37 ; N, 12.38

solubility : hot DMSO

Λ_M (DMSO) : 10.3 $ohm^{-1}cm^2mol^{-1}$

(4) $[Co_2([20]\text{-DCHDC})(NCS)_2] \cdot 2H_2O$.

A solution of $[Co_2([20]\text{-DCHDC})Cl_2] \cdot 2H_2O$(0.707 g) in hot water (100 mL) was added dropwise a solution of sodium thiocyanide (0.49 g) in water (30 mL) with stirring and the mixture was refluxed for 4 h. The resulting dark brown precipitate were filtered, thoroughly washed twice with water, and dried under vacuum.

Yield : 0.6963 g (92.5%)

Anal. Calc.(%) for $Co_2(C_{30}H_{34}N_4O_2)(NCS)_2(H_2O)_2$

C, 51.07 ; H, 5.09 ; N, 11.17

Found(%) C, 51.12 ; H, 5.13 ; N, 11.99

solubility : hot DMSO, hot DMF

λ_M (DMSO) : 39.5 $ohm^{-1}cm^2mol^{-1}$

(5) $[Co_2([20]\text{-}DCHDC)(NO_2)_2] \cdot 3.5H_2O$.

A solution of $[Co_2([20]\text{-}DCHDC)Cl_2] \cdot 2H_2O$(0.707 g) in hot water (100 mL) was added dropwise a solution of sodium nitrite (0.69 g) in water (30 mL) with stirring and the mixture was refluxed whereupon the initial red-brown precipitate first turned dark orange. The resulting dark brown precipitate were filtered, thoroughly washed twice with water, and dried under vacuum.

Yield : 0.5604 g (74.2%)

Anal. Calc.(%) for $Co_2(C_{30}H_{34}N_4O_2)(NO_2)_2(H_2O)_{3.5}$

C, 47.69 ; H, 5.47 ; N, 11.12

Found(%) C, 47.70 ; H, 5.36 ; N, 11.89

solubility : hot DMSO

λ_M (DMSO) : 54.3 $ohm^{-1}cm^2mol^{-1}$

(6) $[Co_2([20]\text{-}DCHDC)(OH_2)_4](NO_3)_2$.

A solution of $[Co_2([20]\text{-}DCHDC)Cl_2] \cdot 2H_2O$(0.707 g) in hot water (100 mL) was added dropwise a solution of sodium nitrate (0.849 g) in water (30 mL) with stirring and the mixture was refluxed for 4 h. The resulting dark brown precipitate were filtered, thoroughly washed twice with water, and the filtrate was on standing in beaker at room temperature. After two days, dark brown crystal was obtained, filtered-off, washed twice with water and dried under vacuum.

Yield : 0.1150 g (14.4%)

Anal. Calc.(%) for $Co_2(C_{30}H_{34}N_4O_2)(NO_3)_2(H_2O)_4$

C, 45.24 ; H, 5.31 ; N, 10.55

Found(%) C, 45.15 ; H, 5.57 ; N, 11.18

solubility : hot DMSO

λ_M (DMSO) : 160.8 $ohm^{-1}m^2mol^{-1}$

(7) $[Co_2([20]\text{-DCHDC})(N_3)_3(OH)]$.

A solution of $[Co_2([20]\text{-DCHDC})Cl_2] \cdot 2H_2O$(0.707 g) in hot water (100 mL) was added dropwise a solution of sodium azide (0.65 g) in water (30 mL) with stirring and the mixture was refluxed for 6h. The resulting dark brown precipitate were filtered, thoroughly washed twice with water and dried under vacuum.

Yield : 0.6205 g (83.4%)

Anal. Calc.(%) for $Co_2(C_{30}H_{34}N_4O_2)(N_3)_3(OH)$

C, 48.46 ; H, 4.74 ; N, 24.49

Found(%) C, 48.74 ; H, 4.49 ; N, 24.51

solubility : hot DMSO

λ_M (DMSO) : 5.3 $ohm^{-1}cm^2mol^{-1}$

III. Results and Discussion

1. Synthesis and characterization of the macrocyclic ligand with 2,6-diformyl -*p*-cresol and *trans*-1,2-diaminocyclohexane

Synthesis and study of new ligands with phenolic groups is an area of active research interest because of their use as models for biological metal-binding sites, their ability to form metal complexes with interesting magnetic exchange, redox and catalytic properties. 2,6-Diformyl-*p*-cresol is a useful source to synthesise such ligands and oxo-bridged macrocyclic complexes with diamines in the presence of template metal salts. Preformed ligands are required to investigate host-guest interactions, to synthesise complexes of metals inert to template reactions and complexes of heteronuclear metals.

The reaction of 2,6-diformyl-*p*-cresol and trans-1,2-diaminocyclohexane in methanol in equimolar ratio using the high dilution technique affords a [3 + 3] Schiff-base macrocycle L_3 as yellow solid in high yield. The CHN, IR, NMR and FAB mass spectral data of the product do not agree with the expected a [2 + 2] Schiff-base macrocycle ligand L_2(=H_2[20]-DCHDC) but match with the composition of [3 + 3] Schiff-base macrocycle L_3 (Scheme 2).

The molecular ion peak at m/z 727 in the FAB mass spectra of L_3 indicates the condensation of three units of 2,6-diformyl-*p*-cresol and three units of trans-1,2-diaminocyclohexane (Figure. 1).

The 400 MHz ($CDCl_3$) ^{1}H NMR spectrum of the ligand, depicted in Figure. 2, consists of a singlet at 8.670, 8.210, 7.576, and 6.898 ppm due to the

azomethine N=CH- and cresol aromatic protons, respectively. The singlet at 2.079 ppm is due to the Ar-CH_3 protons. The multilet at 3.383 and 1.845 -1.469 ppm are due to the N-CH and CH_2CH_2 protons of cyclohexane, respectively. The 100 MHz ($CDCl_3$) ^{13}C NMR spectrum (Figure. 3) of the ligand, depicted in Fig. 2, consists of 14 peaks (19.98, 24.40, 33.15, 33.45, 73.29, 75.36, 118.77, 122.959, 126.84, 129.62, 134.21, 156.18, 159.46, 163.46).

Infrared spectra (Figure. 4) of the ligand show *ν*(C=N) stretching vibration bands at around 1638 cm^{-1} and the absence of any carbonyl bands associated with the diformyl-phenol starting materials or nonmarcrocyclic intermediates. The IR spectra displayed three C-H stretching vibrations from 3018 to 2856 cm^{-1}. A strong bands at near ~1600 cm^{-1} region associated with the aromatic ring C=C vibrations. The sharp absorption bands occurring at ~1258 cm^{-1} are attributed to phenolic C-O stretching vibration. The present complexes exhibited four C-H deformation bands at 1447, 1390, 1371 and 1312 cm^{-1} regions and three out-of-plan vibration bands at 868, 827 and 761 cm^{-1} regions. The broad band occurring in the IR spectra of the complexes in the ~3439 cm^{-1} regions may probably be due to the *ν*(OH) vibration of the phenol and lattice water.

The electronic absorption spectrum of the free ligand H_2[20]-DCHDC in DMF was represented in Figure. 5. The absorption band at 450 nm (ε = 474 $M^{-1}cm^{-1}$) is associated with π-π^* transitions of conjugated [3 + 3] macrocyclic ligand. [30]

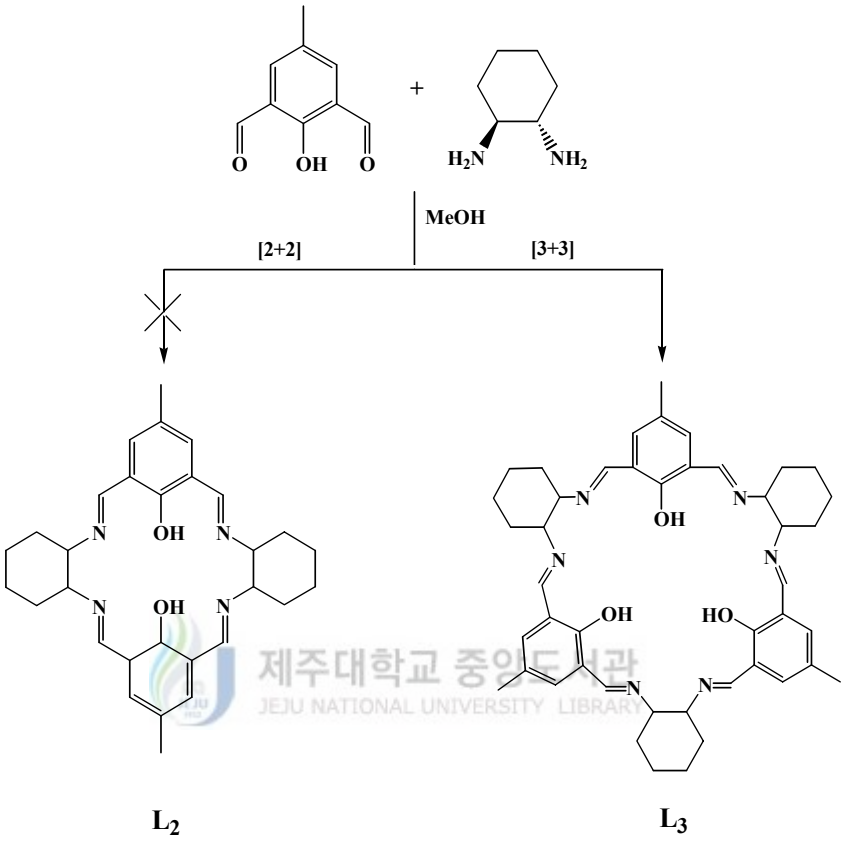

Scheme 2. Product formation pattern of macrocyclic ligand with 2,6-diformyl -*p*-cresol and *trans*-1,2-diaminocyclohexane.

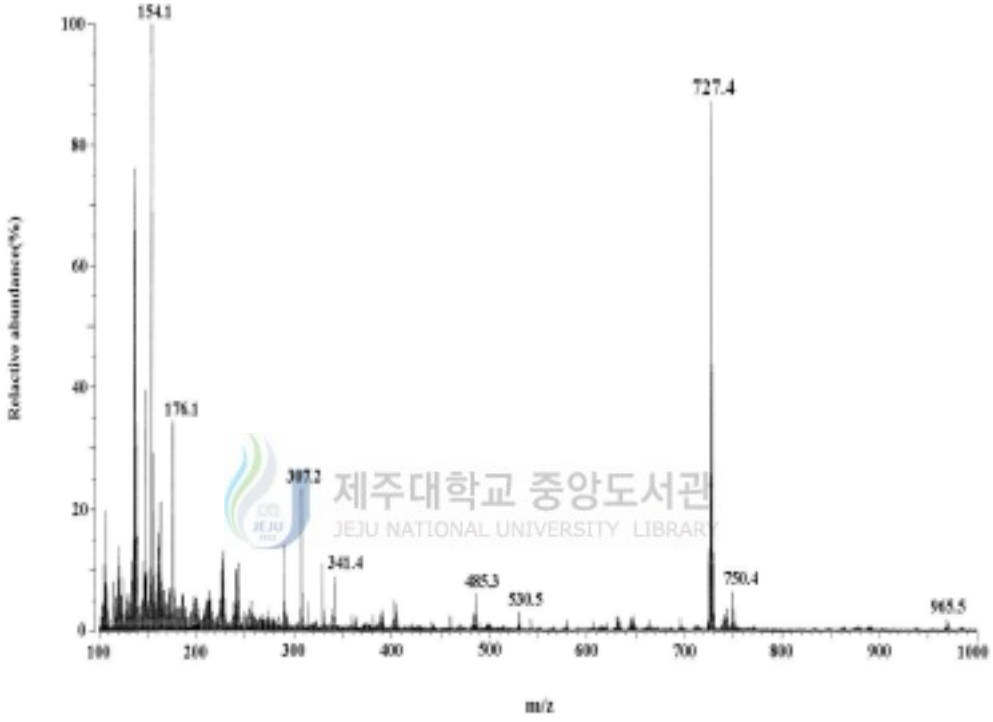

Figure. 1. FAB-mass spectrum of the [3 + 3] Schiff-base macrocycle L_3 ligand.

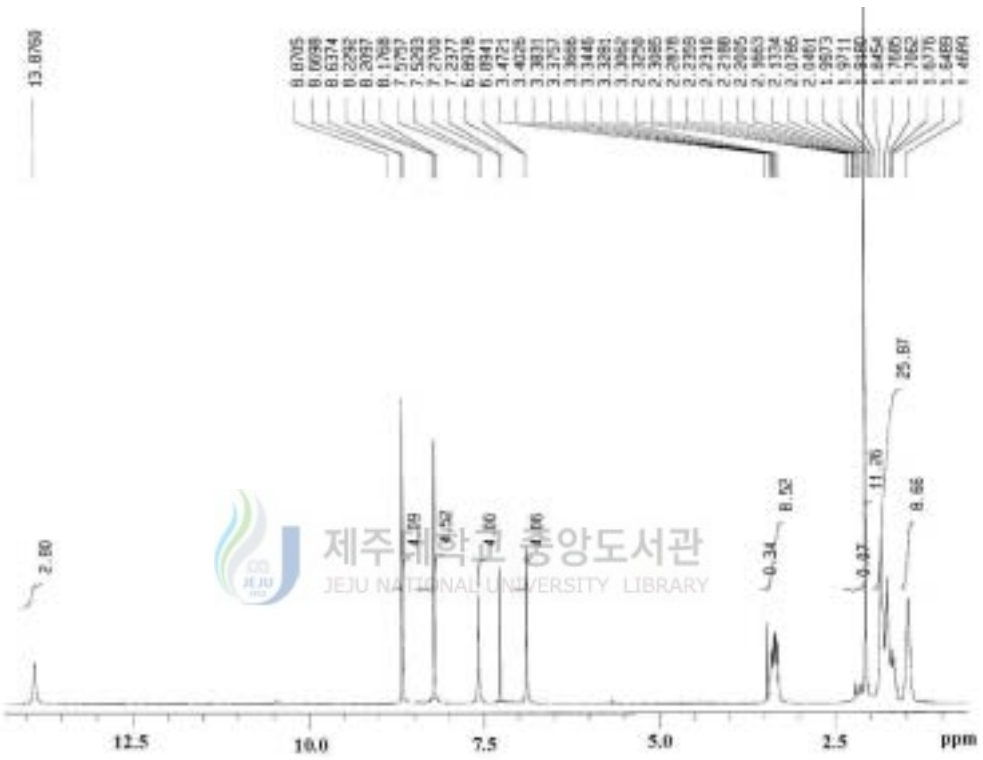

Figure. 2. ^{1}H-NMR spectrum of the [3 + 3] Schiff-base macrocycle L_3 ligand (solvent : $CDCl_3$).

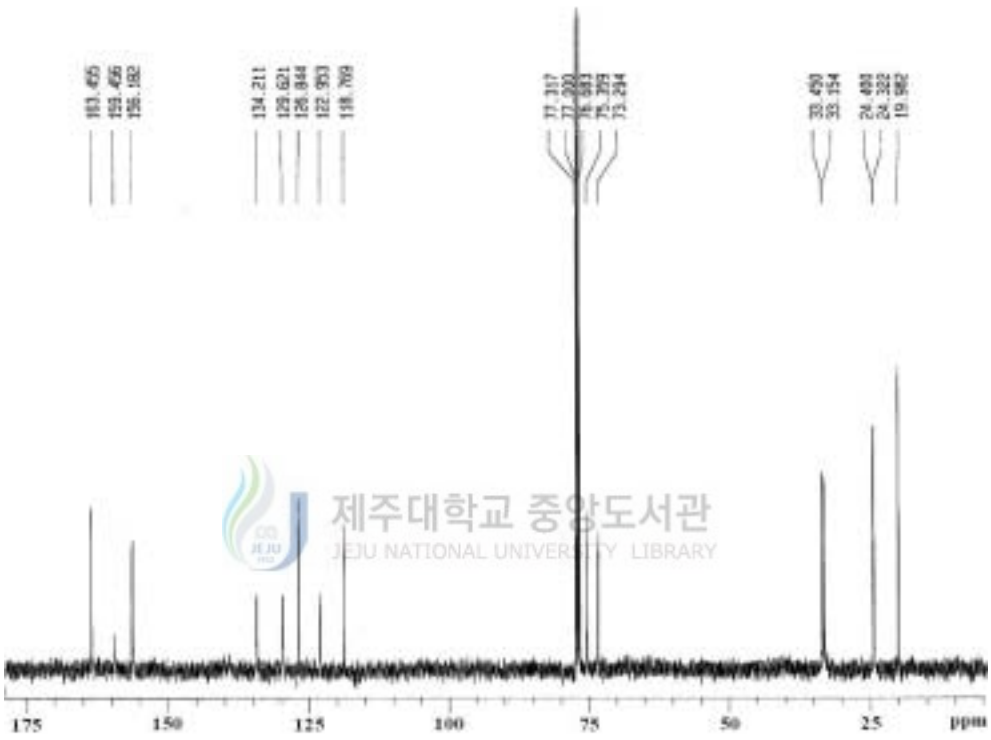

Figure. 3. ^{13}C-NMR spectrum of the [3 + 3] Schiff-base macrocycle L_3 ligand (solvent : $CDCl_3$).

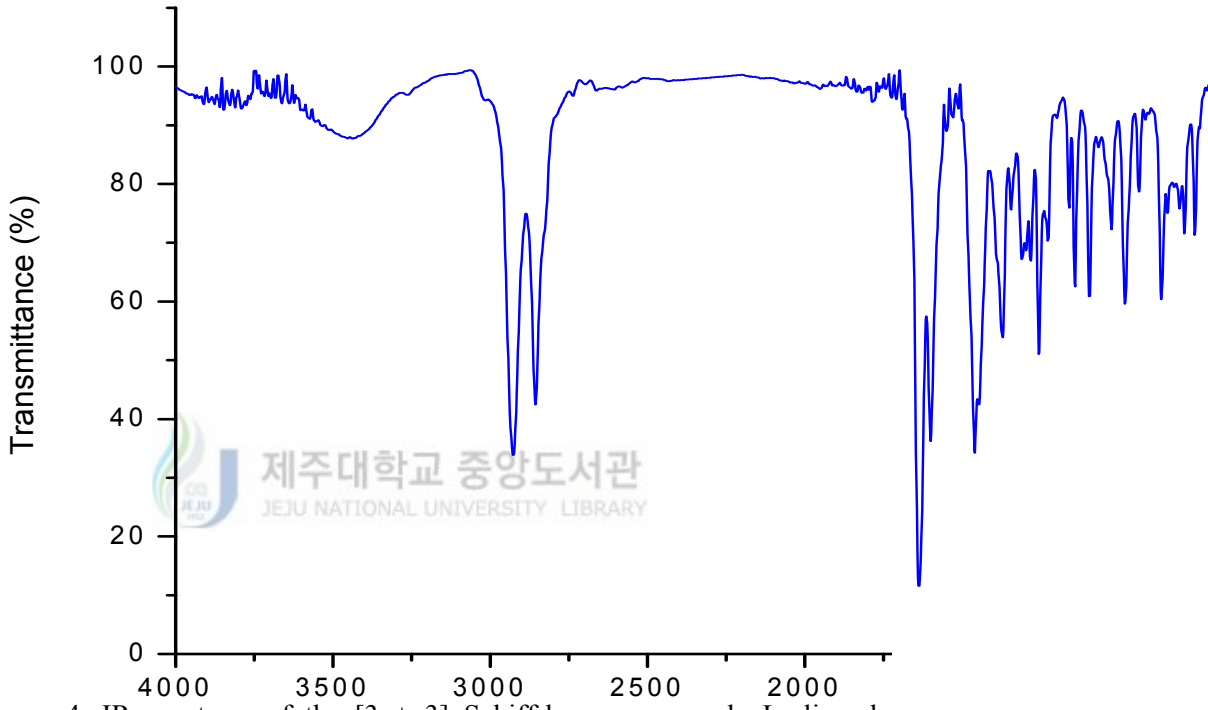

Figure. 4. IR spectrum of the [3 + 3] Schiff-base macrocycle L_3 ligand.

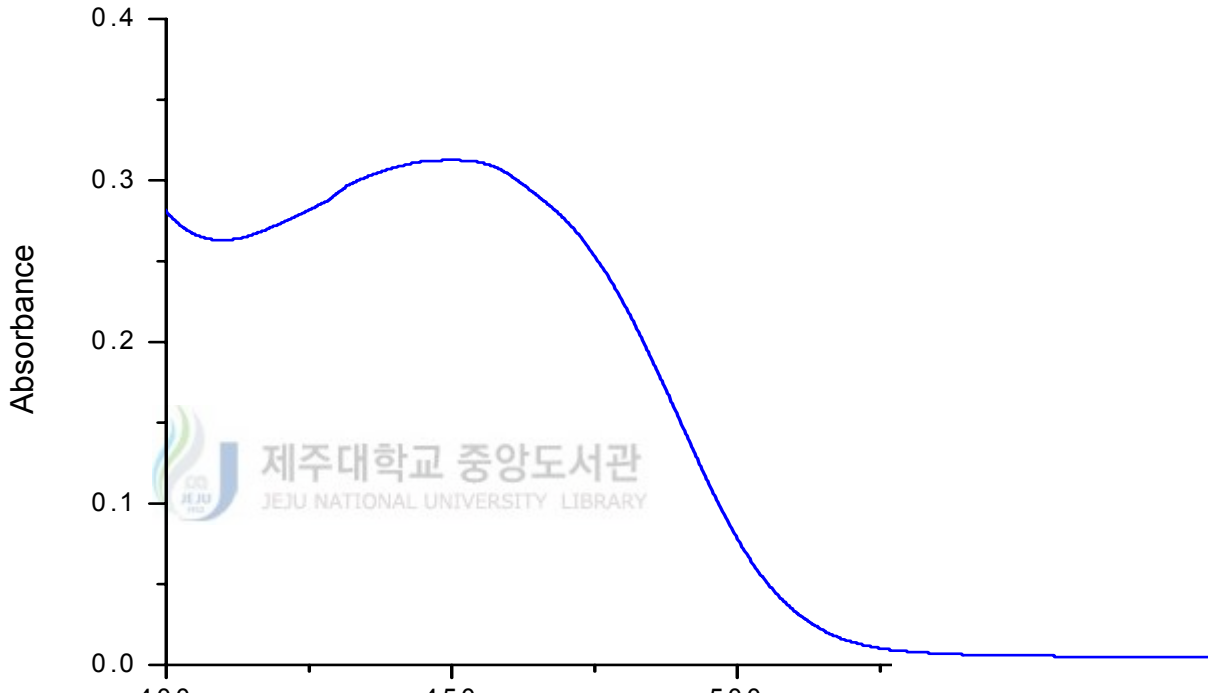

Figure. 5. Electronic absorption spectrum of the [3 + 3] Schiff-base macrocycle L_3 ligand in DMF.

2. IR spectra of the complexes

IR spectra of the cobalt complexes were presented in Figure. 6～12. The characteristics of the complexes were listed in Table 1 and 2. The strong and sharp absorption bands occurring at 1632～1643 cm^{-1} are attributed to ν(C=N) of the coordinated [(H_2[20]-DCHDC)] ligand [31, 32], and the absence of any carbonyl bands associated with the diformylphenol starting materials or nonmarcrocyclic intermediates. The IR spectra displayed three C-H stretching vibrations from 3050 to 2800 cm^{-1}. A strong bands at near ～1550 cm^{-1} region associated with the aromatic ring C=C vibrations. The sharp absorption bands occurring at ～1230 cm^{-1} are attributed to phenolic C-O stretching vibration. The present complexes exhibited four C-H deformation bands at 1450, 1380, 1350 and 1310 cm^{-1} regions and three out-of-plan vibration bands at 870, 820 and 760 cm^{-1} regions. The bands occurring in the IR spectra of the complexes in the 3500～3300 cm^{-1} regions may probably be due to the ν(OH) vibration of the coordinated and/or lattice water.

The perchlorate ion may coordinate to a metal atom as a unidentate ligand M-$OClO_3$, as a chelating bidentate ligand

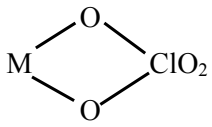

or as a bridging bidentate ligand M-O-ClO_2-O-M. Free ClO_4^- ion with tetrahedral symmetry, T_d, have four fundamental vibrations, only two of which are infrared active (one stretching mode and bending mode). For unidentate coordination

(M-$OClO_3$), the symmetry is reduced to C_{3v}, each of the bands for the free ion being split into two bands with, in addition, the two previously only Raman active vibrations now becoming infrared active. Therefore, three bands due to stretching vibrations and three due to bending vibrations are expected. For bidentate coordination (M-O_2ClO_2 and M-O-ClO_2-O-M), the symmetry is reduced to C_{2v} and each of the bands due to the two modes of vibration of the free ion is now split into three, so that, taking into account the bands which were inactive for the free ion, four bands due to stretching vibrations and four due to bending vibrations are observed [33]. The strong four bands at 1146, 1121, 1109, and 1089 cm^{-1} in $[Co_2([20]\text{-DCHDC})(\mu\text{-}O_2ClO_2)_2] \cdot H_2O$ complex are attributed to a bridging bidentate ligand Co-O-ClO_2-O-Co. The complex exhibited two ClO_4^- deformation bands at 636 cm^{-1} and 627 cm^{-1} regions.

In metal-cyano complexes, the C≡N group may act as a terminal or bridging group. Terminal C≡N groups exhibit a sharp band in the region 2250～2000 cm^{-1} whereas bridging C≡N groups absorb near 2130 cm^{-1}[34]. Absorption bands are also observed in the ranges of 570-180 cm^{-1} and 450-295 cm^{-1}. Cyano complexes exhibit bands due to M-C stretching in the region 600-350 cm^{-1}, due to M-CN deformation in the region 130-60 cm^{-1}. In aqueous solution, the free CN^- ion absorbs near 2080 cm^{-1} (general range, 2250-2000 cm^{-1}, covalently bonded cyanide compounds absorb in the region 2250-2170 cm^{-1}). The CN^- ion may coordinate to a metal atom by σ-donation, which increases the frequency of the CN stretching vibration, or by π-donation from the metal, which reduces the CN stretching frequency. Since CN^- is a good σ-donor and a poor π-acceptor, the CN stretching frequency generally increases on coordination. The absorption peak at 2125 cm^{-1} in the $[Co_2([20]\text{-DCHDC})(CN)_2] \cdot 2H_2O$ is assigned to the

stretching frequency of CN.

The thiocyanate ion may act as an ambidentate ligand, bonding may occur either through the nitrogen or the sulphur atom. The bonding mode may easily be distinguished by examining the band due to the C-S stretching vibration which occurs at 730-690 cm^{-1} when the bonding occurs through the sulphur atom and at 860-780 cm^{-1} when it is through the nitrogen atom[35]. The C≡N stretching vibration of thiocyanato-complexes (sulphur-bound, i.e. M-SCN) gives rise to a sharp band at about 2100 cm^{-1} and Ga-NCS (i.e. nitrogen bound), the resulting band is often broad and occurs near and below 2050 cm^{-1}. The absorption vibrations due to the N-coordinated bonded NCS^- in $[Co_2([20]\text{-DCHDC})(NCS)_2] \cdot 2H_2O$ appear 2071 and 837 cm^{-1}.

Linkage isomerism is possible in the case of metal complexes containing the unit NO_2. Coordination to the metal atom may occur through the nitrogen atom, resulting in a nitro-complex, or through an oxygen atom, resulting in a nitrito-complex. Nitro-complexes exhibit bands due to asymmetric and symmetric -NO_2 stretching vibration and, in addition, one due to a NO_2 deformation vibration.[35] The nitrito-complexes exhibit bands due to asymmetric and symmetric -ONO stretching vibrations which are well separated and occur at 1485-1400 cm^{-1} and 1110-1050 cm^{-1}, respectively. Nitro-groups in metal coordination complexes may exist as bridging or as end groups. Terminal nitro-groups absorb at 1485-1370 cm^{-1} and 1340-1315 cm^{-1} due to the asymmetric and symmetric stretching vibrations of the NO_2 group, respectively[35, 37]. Nitrito-complexes do not have a band near 620cm^{-1} which is present for all nitro-complexes. Nitro- groups acting as bridging units between two metal atoms absorb at 1485-1470cm^{-1} and at about 1200cm^{-1}, these bands

being broader than those for terminal nitro- groups. The very strong absorption peaks at 1452 and 1312 cm^{-1} in the $[Co_2([20]\text{-}DCHDC)(NO_2)_2] \cdot 3.5H_2O$ are assigned to the antisymmetric and symmetric stretching mode of N-bonded NO_2, respectively. And deformation band of N-bonded NO_2 is observed at 654 cm^{-1}.

The absorption bands of coordinate nitrate occurring in the IR spectra of $[Co_2([20]\text{-}DCHDC)(OH_2)_4](NO_3)_2$ in the 1454, 1313 and 1038 cm^{-1} regions are assignable to the ν(N=O) (ν_1), $\nu_a(NO_2)$ (ν_5) and $\nu_s(NO_2)$ (ν_2) vibrations, respectively. The very strong absorption band at 1385 cm^{-1} is characteristic of ionic nitrate present in the outer-coordination sphere [33].

In general, for azides the band due to the asymmetric N_3 stretching vibration is strong and occurs in the region 2195-2030 cm^{-1}, while that due to the symmetric vibration is much weaker and occurs in the region 1375-1175 cm^{-1} and the band due to the deformation vibration is also weak and occurs at 680-410 cm^{-1} [36]. The absorption peaks at 2034 and 2010 cm^{-1} in the $[Co_2([20]\text{-}DCHDC)(N_3)_3(OH)]$ are assigned to the asymmetric stretching mode of coordinated azide. The symmetric stretching frequency of coordinated azide is observed at 1286 cm^{-1}. And deformation band of coordinated azide is observed at 652 cm^{-1}. The stretching vibration band near 3471 cm^{-1}, and the band due to the deformation vibration is also weak and occurs at 1037 cm^{-1}. These bands occurring in the IR spectra, may probably be due to the ν(OH) vibration of the coordinated hydroxo complexes Co-OH.

Table 1. Characteristic IR absorptions (cm^{-1}) of macrocyclic ligand for the dinuclear Cobalt complexes

Compounds	Assignments					
	Macrocycle					
	ν(CH)			ν(C=N)	ν(C=C)	ν(C-O)
$[Co_2([20]\text{-DCHDC})Cl_2] \cdot 2H_2O$	3030 (w)	2937 (m)	2860 (m)	1638 (vs)	1552 (s)	1238 (m)
$[Co_2([20]\text{-DCHDC})(\mu\text{-}O_2ClO_2)_2] \cdot H_2O$	3055 (w)	2937 (m)	2860 (m)	1643 (vs)	1554 (s)	1240 (m)
$[Co_2([20]\text{-DCHDC})(CN)_2] \cdot 2H_2O$	3032 (w)	2939 (s)	2862 (s)	1639 (vs)	1541 (vs)	1236 (s)
$[Co_2([20]\text{-DCHDC})(NCS)_2] \cdot 2H_2O$	3024 (w)	2939 (m)	2862 (m)	1631 (vs)	1550 (vs)	1236 (s)
$[Co_2([20]\text{-DCHDC})(NO_2)_2] \cdot 3.5H_2O$	3044 (w)	2934 (m)	2862 (m)	1633 (s)	1553 (s)	1236 (m)
$[Co_2([20]\text{-DCHDC})(OH_2)_4](NO_3)_2$	3036 (w)	2936 (m)	2860 (m)	1639 (s)	1553 (s)	1236 (s)
$[Co_2([20]\text{-DCHDC})(N_3)_3(OH)]$	3028 (w)	2936 (m)	2862 (m)	1632 (s)	1549 (s)	1236 (m)

Compounds	Assignments						
	Macrocycle						
	δ(CH)				δ_{oop}(CH)		
$[Co_2([20]\text{-DCHDC})Cl_2] \cdot 2H_2O$	1450 (m)	1383 (m)	1360 (m)	1311 (m)	870 (w)	823 (w)	770 (w)
$[Co_2([20]\text{-DCHDC})(\mu\text{-}O_2ClO_2)_2] \cdot H_2O$	1454 (m)	1383 (m)	1352 (m)	1312 (m)	871 (w)	825 (w)	767 (w)
$[Co_2([20]\text{-DCHDC})(CN)_2] \cdot 2H_2O$	1454 (s)	1383 (s)	1350 (s)	1308 (m)	871 (m)	823 (m)	770 (m)
$[Co_2([20]\text{-DCHDC})(NCS)_2] \cdot 2H_2O$	1452 (s)	1381 (m)	1348 (m)	1308 (m)	871 (w)	824 (m)	767 (w)
$[Co_2([20]\text{-DCHDC})(NO_2)_2] \cdot 3.5H_2O$	1452 (vs)	1381 (s)	1350 (m)	1312 (vs)	876 (w)	815 (m)	754 (w)
$[Co_2([20]\text{-DCHDC})(OH_2)_4](NO_3)_2$	1454 (m)	1385 (vs)	1358 (s)	1313 (s)	871 (w)	825 (w)	756 (w)
$[Co_2([20]\text{-DCHDC})(N_3)_3(OH)]$	1458 (s)	1383 (m)	1350 (m)	1302 (m)	874 (w)	823 (w)	754 (w)

Table 2. Characteristic IR absorptions (cm^{-1}) of exocycle molecules for the dinuclear Cobalt complexes

Compounds	Assignments
$[Co_2([20]\text{-DCHDC})Cl_2] \cdot 2H_2O$	3425 (br) ; ν(OH) lattice H_2O 459(w); Co-N(macrocycle)
$[Co_2([20]\text{-DCHDC})(\mu\text{-}O_2ClO_2)_2] \cdot H_2O$	3476 (br) ; ν(OH) lattice H_2O 1146(sh), 1121 (s), 1109 (sh), 1089 (sh), bridging ClO_4^- Co-O-ClO_2-O-Co 636(sh), 627(m); coord. ClO_4^- 461(w); Co-N(macrocycle)
$[Co_2([20]\text{-DCHDC})(CN)_2] \cdot 2H_2O$	3437 (br) ; ν(OH) lattice H_2O 2125 (m) ; ν(CN) coord. CN^- 459(w); Co-N(macrocycle)
$[Co_2([20]\text{-DCHDC})(NCS)_2] \cdot 2H_2O$	3464 (br) ; ν(OH) lattice H_2O 2071 (br, vs) ; ν(C=N) N-bonded NCS^- ; 837 (w) ; ν(C-S) N-bonded NCS^- 461(w); Co-N(macrocycle)
$[Co_2([20]\text{-DCHDC})(NO_2)_2] \cdot 3.5H_2O$	3395 ν(OH) lattice H_2O 1383 $\nu_{as}(NO_2)$, 1325 $\nu_s(NO_2)$, 640 $\delta(NO_2)$ N-bonded NO_2^- ; 459(w); Co-N(macrocycle)
$[Co_2([20]\text{-DCHDC})(OH_2)_4](NO_3)_2$	3400 ν(OH) H_2O ; 1384 ionic NO_3^- 459(w); Co-N(macrocycle)
$[Co_2([20]\text{-DCHDC})(N_3)_3(OH)]$	3471 (br) ; ν(OH) hydroxo complexes Co-OH 1037 (w) , δ(OH) Co-OH 2034, 2010 (vs) ; ν_{as}(NNN) coord. N_3^- ; 1286 (m) ; ν_s(NNN) coord. N_3^- ; 652 (w) ; δ(NNN) coord. N_3^- ; 461(w); Co-N(macrocycle)

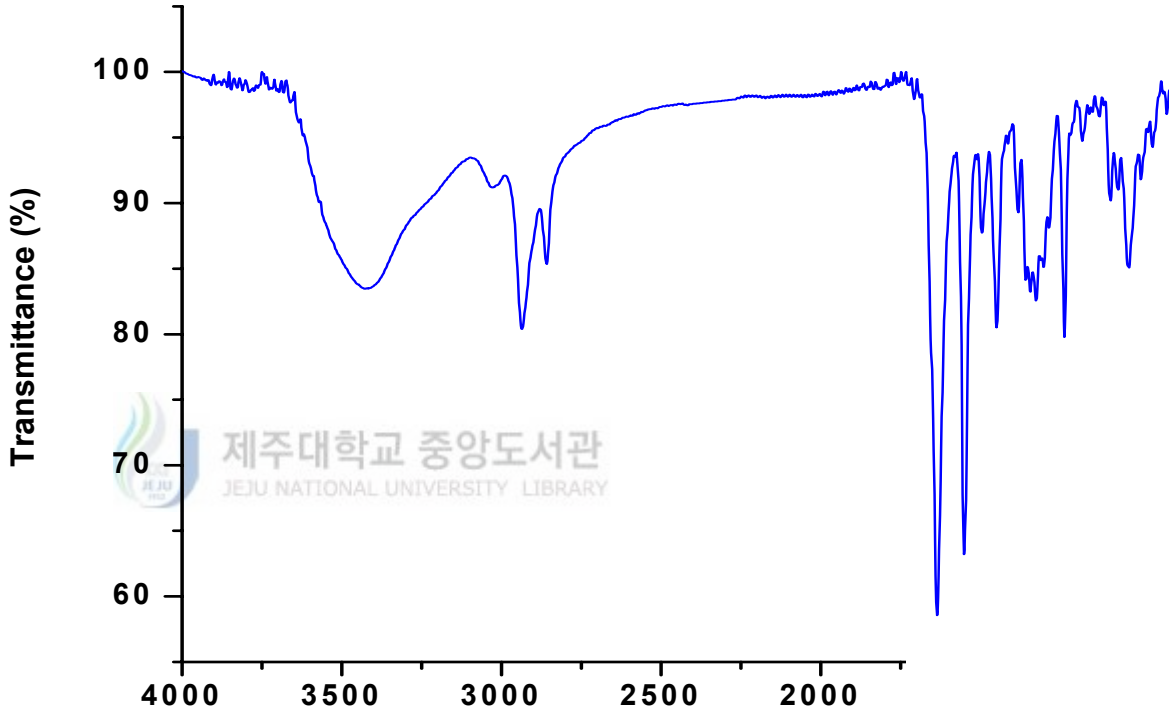

Figure. 6. FT-IR spectrum of $[Co_2([20]\text{-DCHDC})Cl_2] \cdot 2H_2O$.

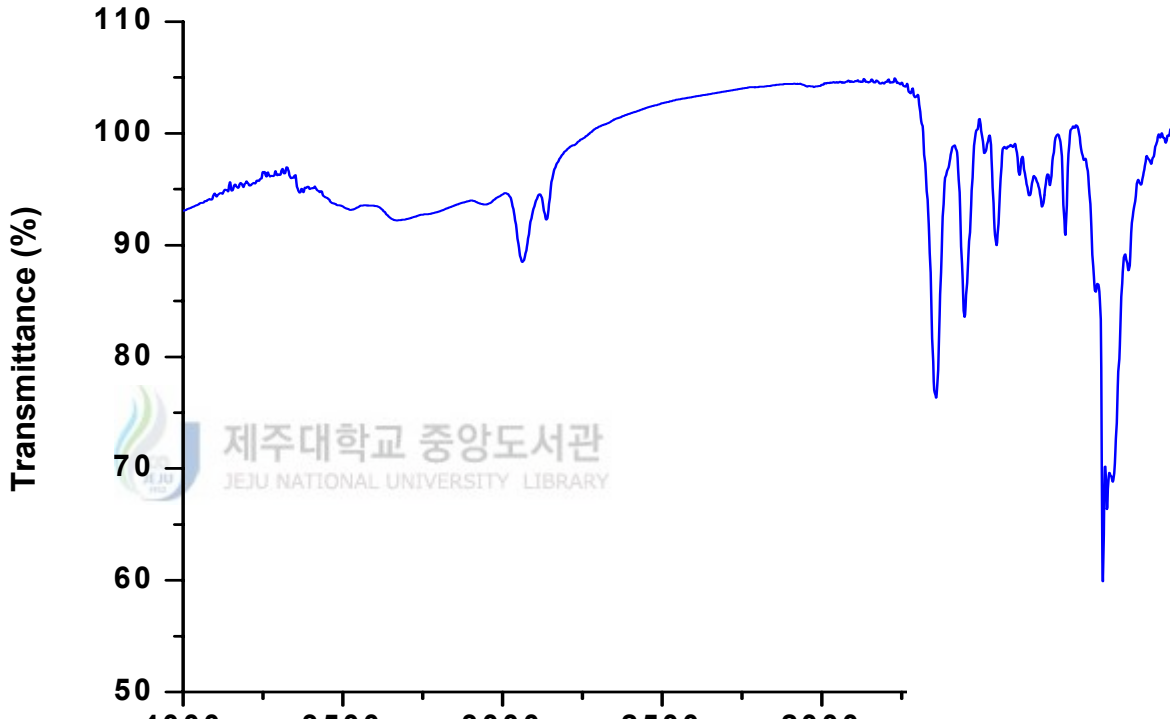

Figure. 7. FT-IR spectrum of $[Co_2([20]\text{-}DCHDC)(\mu\text{-}O_2ClO_2)_2] \cdot H_2O$.

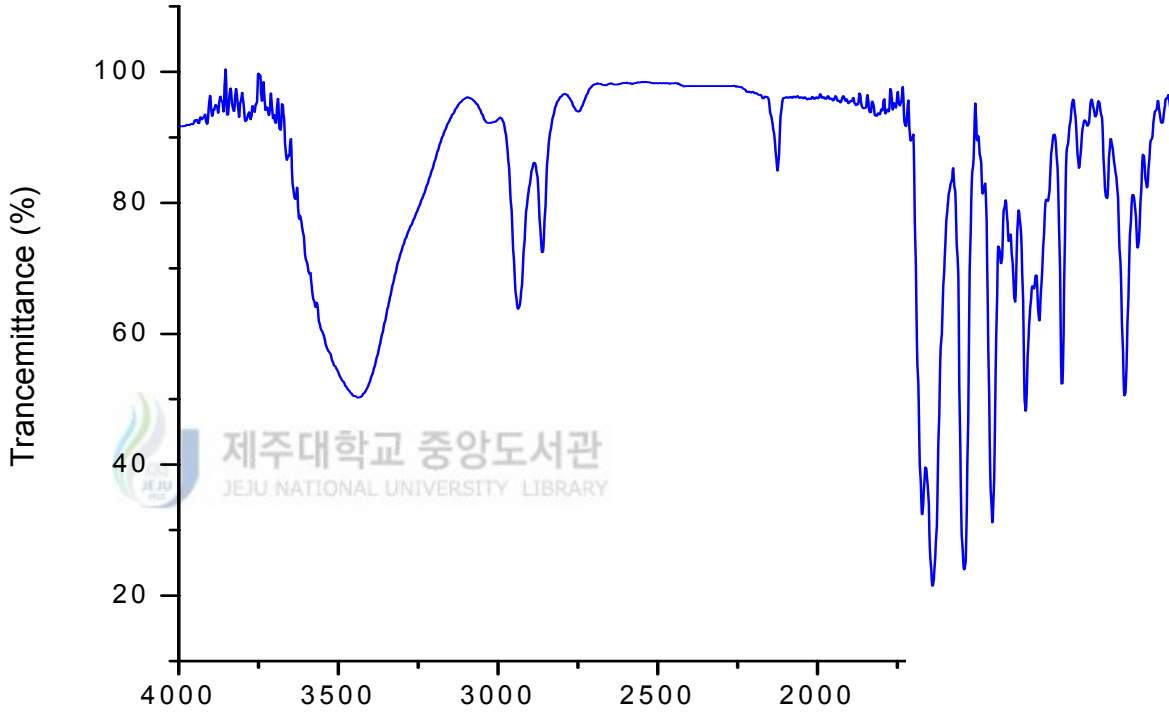

Figure. 8. FT-IR spectrum of $[Co_2([20]\text{-DCHDC})(CN)_2] \cdot 2H_2O$.

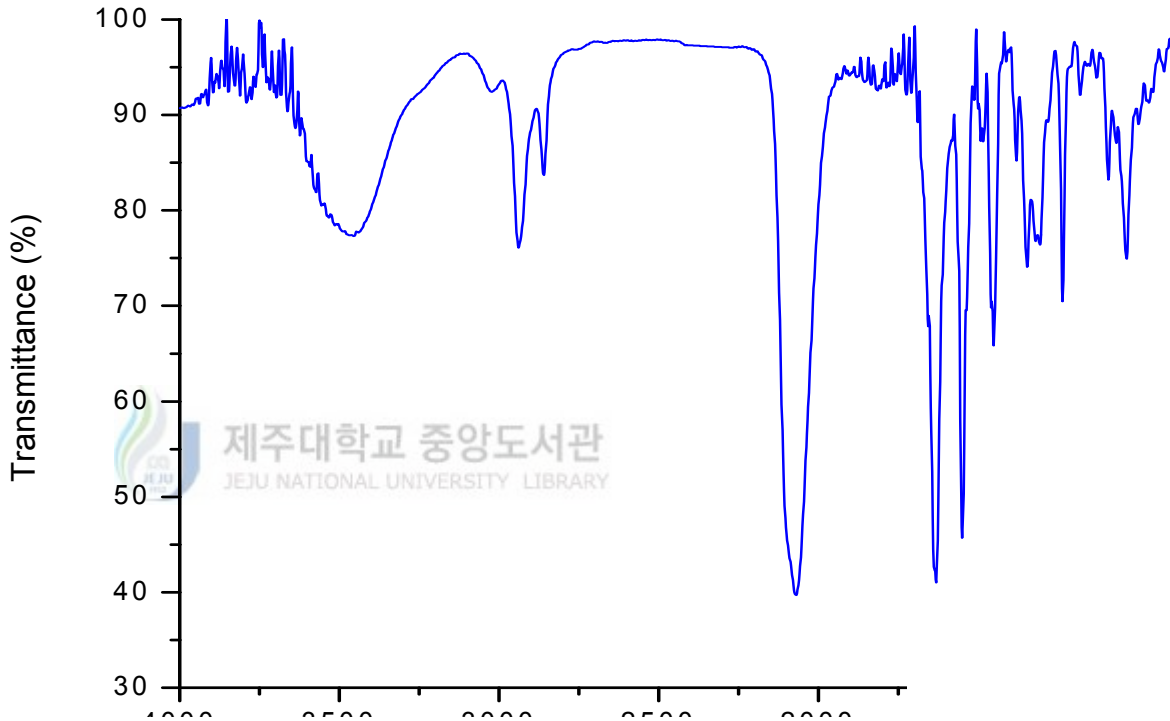

Figure. 9. FT-IR spectrum of $[Co_2([20]\text{-DCHDC})(NCS)_2] \cdot 2H_2O$.

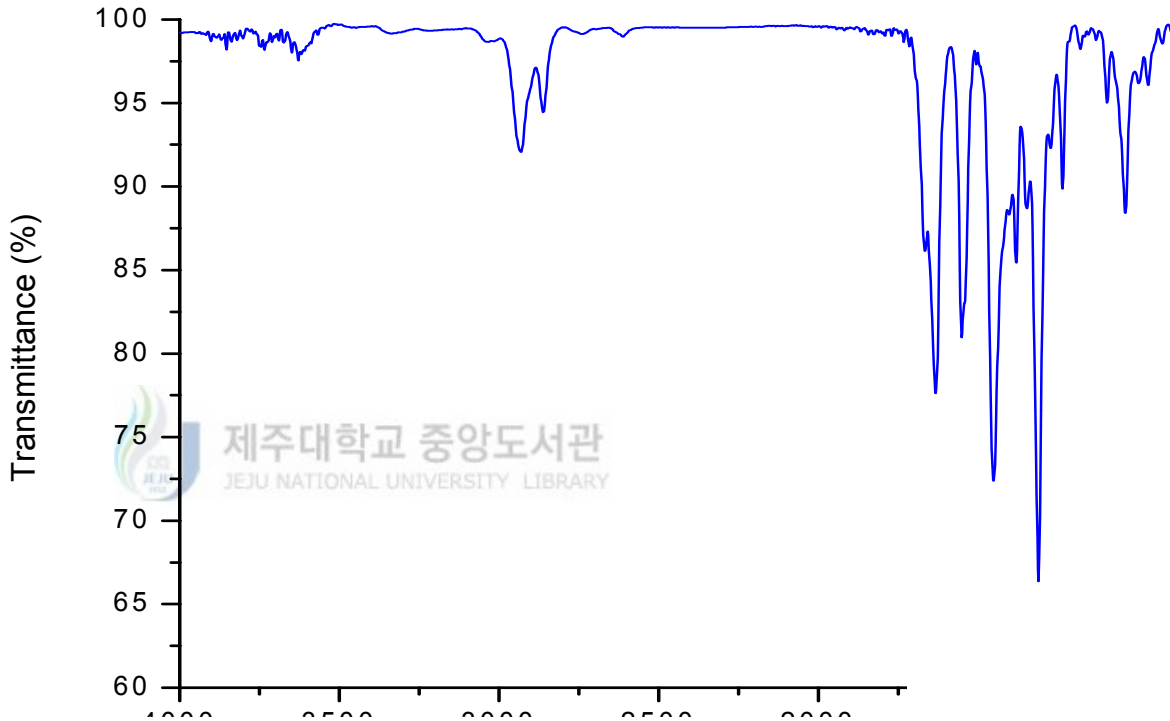

Figure. 10. FT-IR spectrum of $[Co_2([20]\text{-}DCHDC)(NO_2)_2] \cdot 3.5H_2O$.

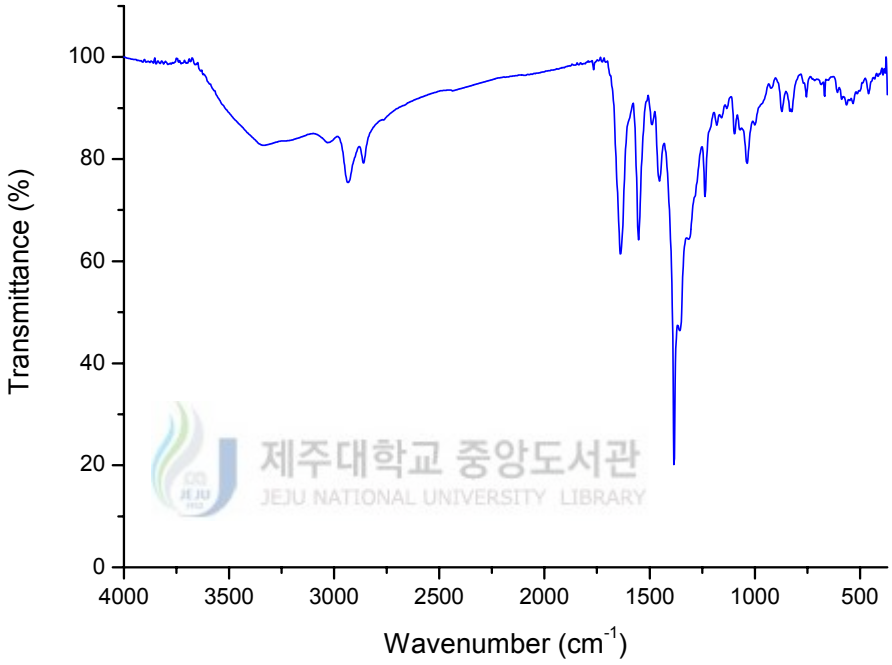

Figure. 11. FT-IR spectrum of $[Co_2([20]\text{-DCHDC})(OH_2)_4](NO_3)_2$.

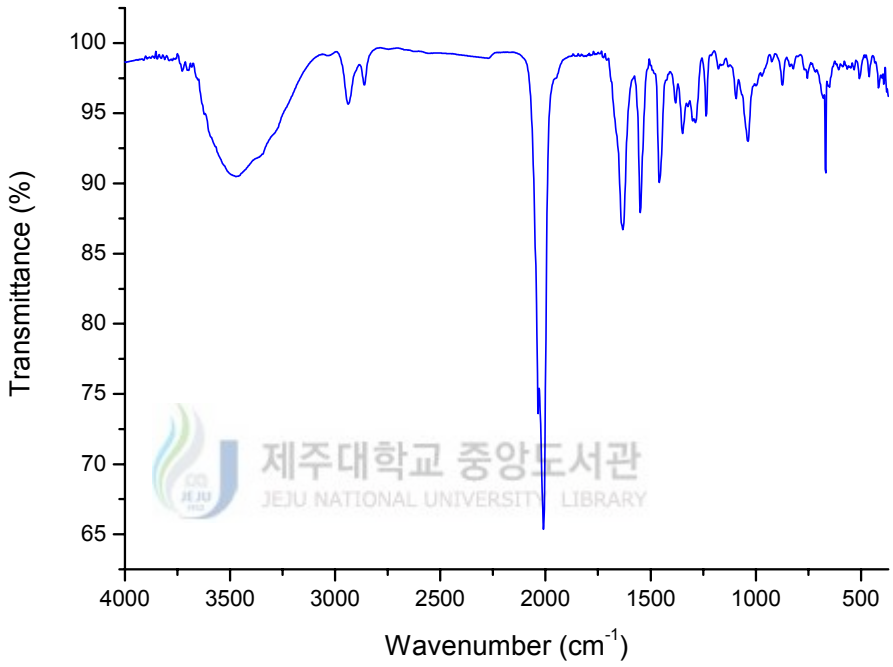

Figure. 12. FT-IR spectrum of $[Co_2([20]\text{-DCHDC})(N_3)_3(OH)]$.

3. FAB-mass spectra of the complexes

The FAB mass spectra of the Cobalt complexes were shown in Figure. 13～19, and summarized at Table 3. The molecular ion loses the exocyclic ligands resulting in the formation of the fragment $[Co_2([20]\text{-}DCHDC)]^+$. All these species are well observed in the FAB mass spectra at m/z 599. α-cleavage peaks of one cyclohexane from the $[Co_2([20]\text{-}DCHDC)]^+$ ion in the formation of the fragment $[Co_2(L_{ac})]^+$ are observed at m/z 518.1 region. Removal peaks of one cobalt ion from the $[Co_2([20]\text{-}DCHDC)]^+$ ion in the formation of the fragment $[Co([20]\text{-}DCHDC)]^+$ is observed at m/z 541. α-cleavage peaks of one cyclohexane from the $[Co([20]\text{-}DCHDC)]^+$ ion in the formation of the fragment $[Co(L_{ac})]^+$ are observed at m/z 461.1 region (Scheme 3).

The FAB mass spectra of all the complexes contain peaks corresponding to the $[(H_2[20]\text{-}DCHDC)]^+$ fragment ion at m/z 489 region. This indicates that the species $[Co_2([20]\text{-}DCHDC)]^+$ undergoes demetallation to give the tetraazadioxa macrocycle H_2[20]-DCHDC under FAB conditions. These peaks are associated with peaks of mass one or two greater or less, which are attributed to protonated /deprotonated forms. This also accounts for the slight ambiguities in making assignments.

The week molecular ion peaks corresponding to the $[Co_2([20]\text{-}DCHDC)\text{-}(ClO_4)]^+$, $[Co_2([20]\text{-}DCHDC)(CN)_2]^+$, $[Co_2([20]\text{-}DCHDC)(NCS)_2]^+$, $[Co_2([20]\text{-}DCHDC)\text{-}(NO_2)_2]^+$, $[Co_2([20]\text{-}DCHDC)(NO_3)]^+$, and $[Co_2([20]\text{-}DCHDC)(N_3)_3(OH)]^+$ are observed at m/z 699.1, 652.1, 716.1, 692.1, 662.1 and 743.2, respectively. Removal peaks of one exocyclic ligand resulting in the formation of the fragment

$[Co_2([20]\text{-DCHDC})(L_a)]^+$ (L_a = Cl^-, CN^-, NCS^- and NO_2^-) are observed at m/z 634.4, 625.5, 657.4 and 645.7, respectively. In the mass spectrum of $[Co_2([20]\text{-DCHDC})(N_3)_3] \cdot H_2O$, the peaks observed at m/z 683.5 and 642.3 are due to fragments $[Co_2([20]\text{-DCHDC})(N_3)_2]^+$ and $[Co_2([20]\text{-DCHDC})(N_3)]^+$, respectively.

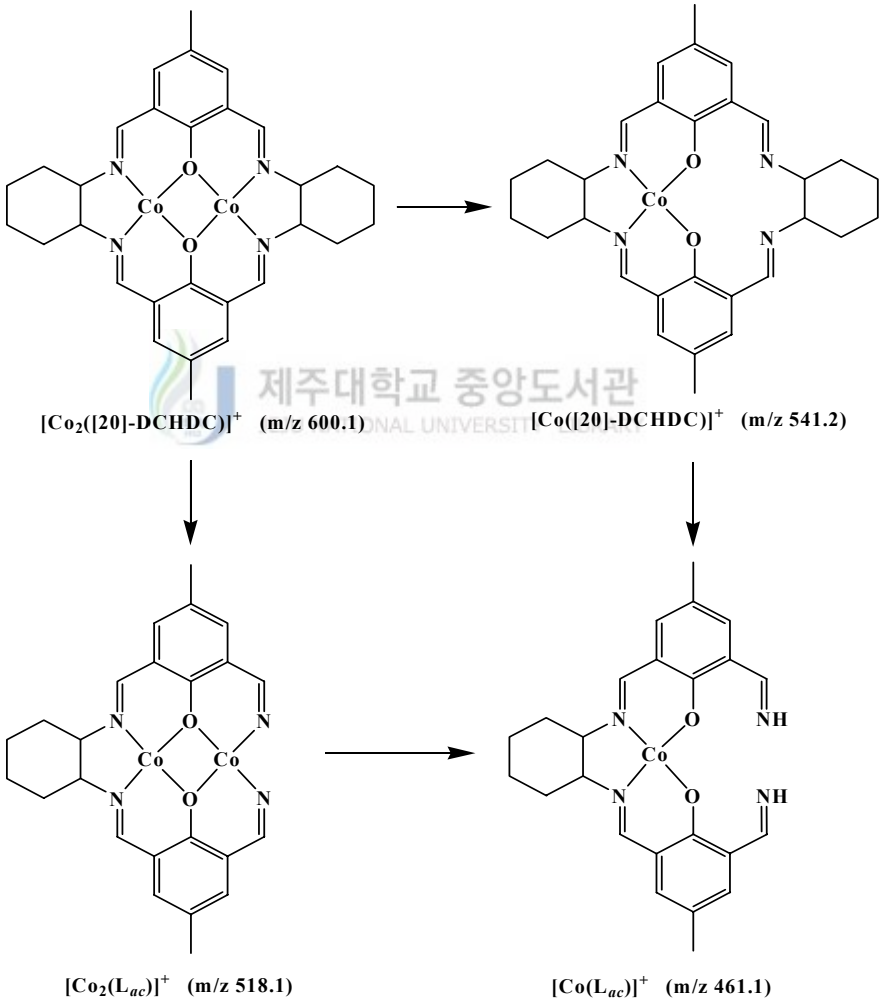

Scheme 3. The fegment pattern of dinuclear Co(ⅡorⅢ) complexes in FAB-mass spectra.

Table 3. FAB-mass spectra for the dinuclear Cobalt complexes of phenol-based macrocyclic ligand (H_2[20]-DCHDC)

complex	m/z	Assignment	
$[Co_2([20]\text{-DCHDC})Cl_2] \cdot 2H_2O$	459.3	$[Co(L_{ac})]^+$	461.1
	489.2	$[(H_2[20]\text{-DCHDC})+5H]^+$	489.3
	517.2	$[Co_2(L_{ac})]^+$	518.1
	541.4	$[Co([20]\text{-DCHDC})]^+$	541.2
	599.4	$[Co_2([20]\text{-DCHDC})]^+$	600.1
	634.4	$[Co_2([20]\text{-DCHDC})(Cl)]^+$	635.1
$[Co_2([20]\text{-DCHDC})(\mu\text{-}O_2ClO_2)_2] \cdot H_2O$	459.5	$[Co(L_{ac})]^+$	461.1
	489.3	$[(H_2[20]\text{-DCHDC})+5H]^+$	489.3
	517.3	$[Co_2(L_{ac})]^+$	518.1
	541.3	$[Co([20]\text{-DCHDC})]^+$	541.2
	599.2	$[Co_2([20]\text{-DCHDC})]^+$	600.1
	698.4	$[Co_2([20]\text{-DCHDC})(ClO_4)]^+$	699.1
$[Co_2([20]\text{-DCHDC})(CN)_2] \cdot 2H_2O$	459.5	$[Co(L_{ac})]^+$	461.1
	485.4	$[(H_2[20]\text{-DCHDC})+H]^+$	485.4
	517.2	$[Co_2(L_{ac})]^+$	518.1
	541.4	$[Co([20]\text{-DCHDC})]^+$	541.2
	599.4	$[Co_2([20]\text{-DCHDC})]^+$	600.1
	625.5	$[Co_2([20]\text{-DCHDC})(CN)]^+$	626.1
	652.4	$[Co_2([20]\text{-DCHDC})(CN)_2]^+$	652.1
$[Co_2([20]\text{-DCHDC})(NCS)_2] \cdot 2H_2O$	459.5	$[Co(L_{ac})]^+$	461.1
	489.3	$[(H_2[20]\text{-DCHDC})+5H]^+$	489.3
	517.2	$[Co_2(L_{ac})]^+$	518.1
	541.3	$[Co([20]\text{-DCHDC})]^+$	541.2
	599.3	$[Co_2([20]\text{-DCHDC})]^+$	600.1
	657.4	$[Co_2([20]\text{-DCHDC})(NCS)]^+$	658.1
	716.4	$[Co_2([20]\text{-DCHDC})(NCS)_2]^+$	716.1

Table 3. *continued*

$[Co_2([20]\text{-}DCHDC)(NO_2)_2]\cdot 3.5H_2O$	459.5	$[Co(L_{ac})]^+$	461.1
	489.3	$[(H_2[20]\text{-}DCHDC)+5H]^+$	489.3
	517.2	$[Co_2(L_{ac})]^+$	518.1
	541.3	$[Co([20]\text{-}DCHDC)]^+$	541.2
	599.3	$[Co_2([20]\text{-}DCHDC)]^+$	600.1
	645.7	$[Co_2([20]\text{-}DCHDC)(NO_2)]^+$	646.1
	691.5	$[Co_2([20]\text{-}DCHDC)(NO_2)_2]^+$	692.1
$[Co_2([20]\text{-}DCHDC)(OH_2)_4](NO_3)_2$	462.4	$[Co(L_{ac})]^+$	461.1
	489.2	$[(H_2[20]\text{-}DCHDC)+5H]^+$	489.3
	517.2	$[Co_2(L_{ac})]^+$	518.1
	541.3	$[Co([20]\text{-}DCHDC)]^+$	541.2
	599.2	$[Co_2([20]\text{-}DCHDC)]^+$	600.1
	661.5	$[Co_2([20]\text{-}DCHDC)(NO_3)]^+$	662.1
$[Co_2([20]\text{-}DCHDC)(N_3)_3(OH)]$	489.3	$[(H_2[20]\text{-}DCHDC)+5H]^+$	489.3
	517.2	$[Co_2(L_{ac})]^+$	518.1
	599.3	$[Co_2([20]\text{-}DCHDC)]^+$	600.1
	642.3	$[Co_2([20]\text{-}DCHDC)(N_3)]^+$	642.1
	683.5	$[Co_2([20]\text{-}DCHDC)(N_3)_2]^+$	684.2
	742.3	$[Co_2([20]\text{-}DCHDC)(N_3)_3(OH)]^+$	743.2

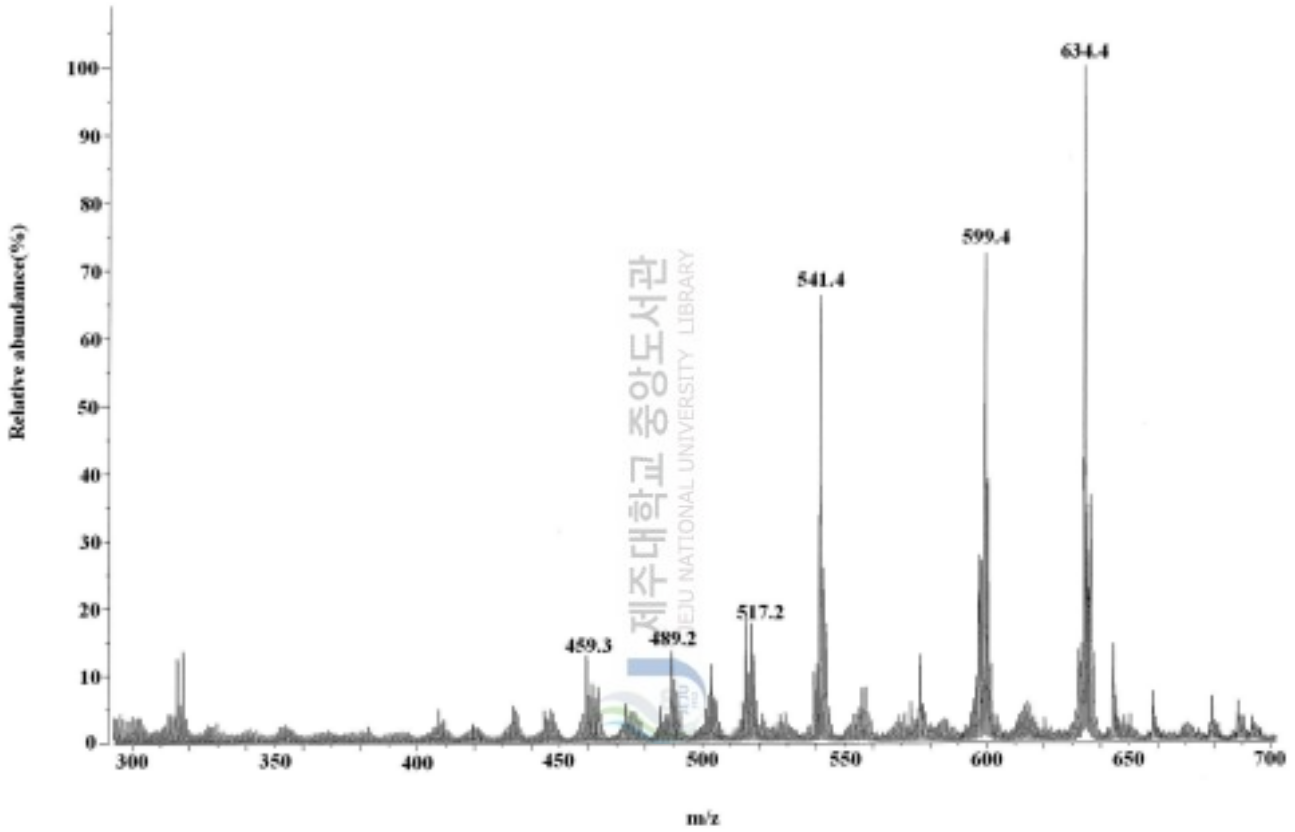

Figure. 13. FAB mass spectrum of the $[Co_2([20]\text{-DCHDC})Cl_2] \cdot 2H_2O$

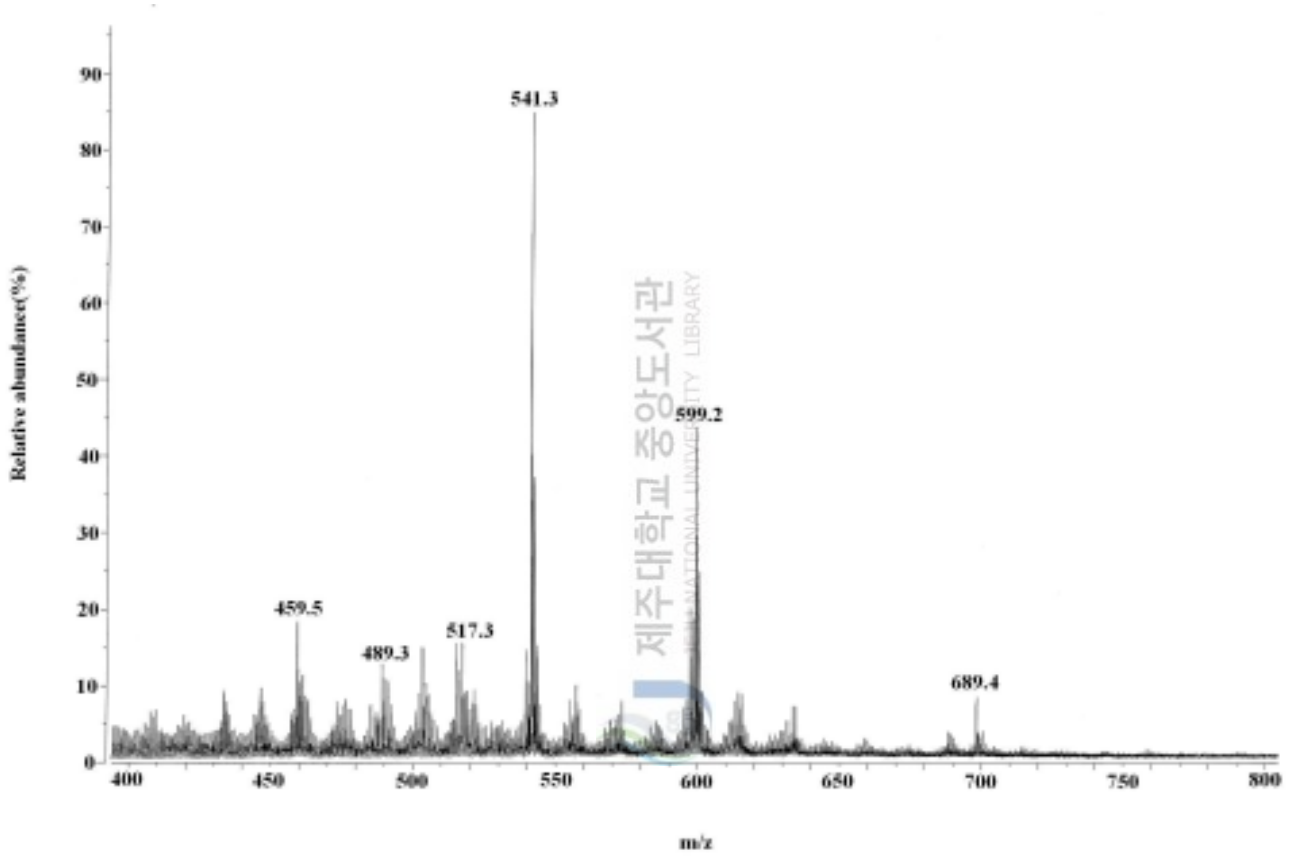

Figure. 14. FAB mass spectrum of the $[Co_2([20]\text{-}DCHDC)(\mu\text{-}O_2ClO_2)_2] \cdot H_2O$.

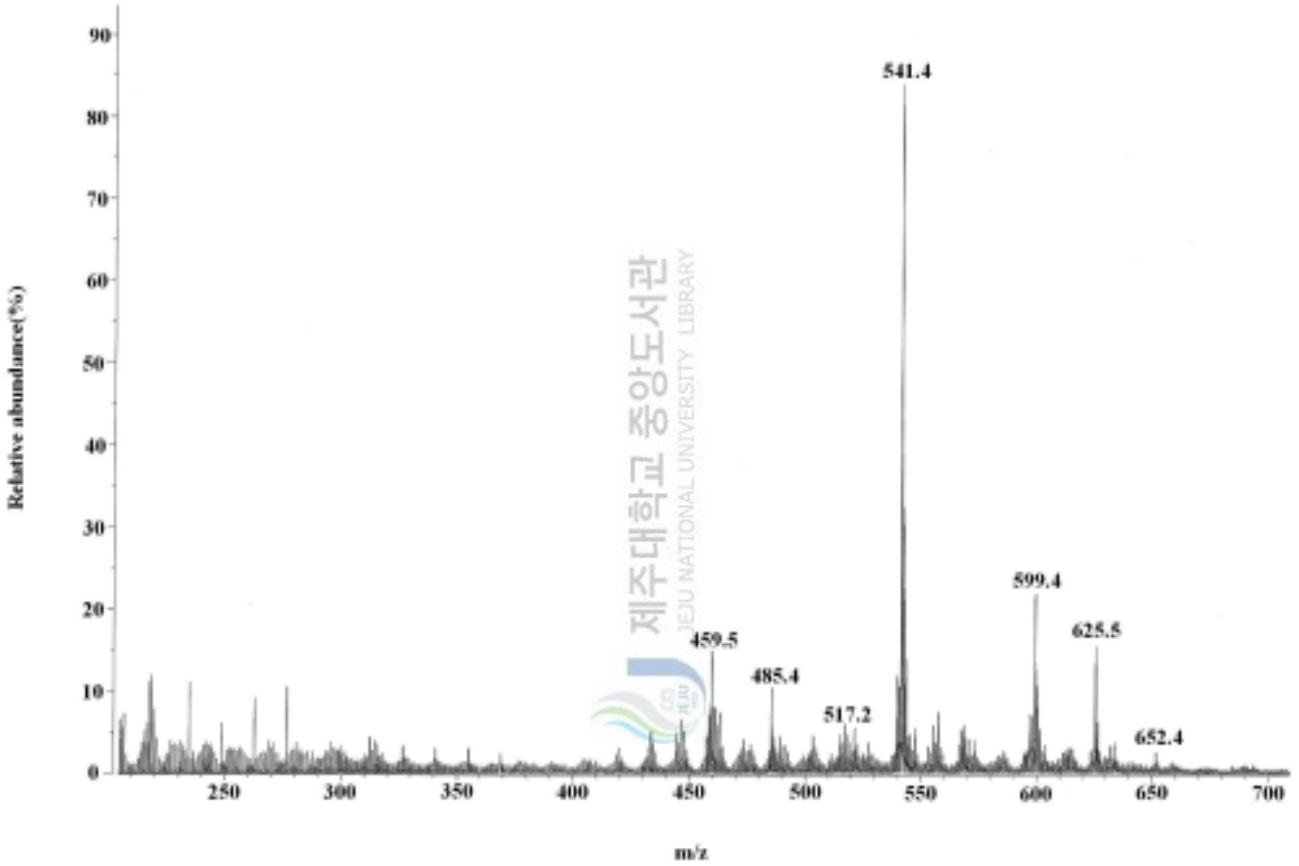

Figure. 15. FAB mass spectrum of the $[Co_2([20]\text{-DCHDC})(CN)_2] \cdot 2H_2O$

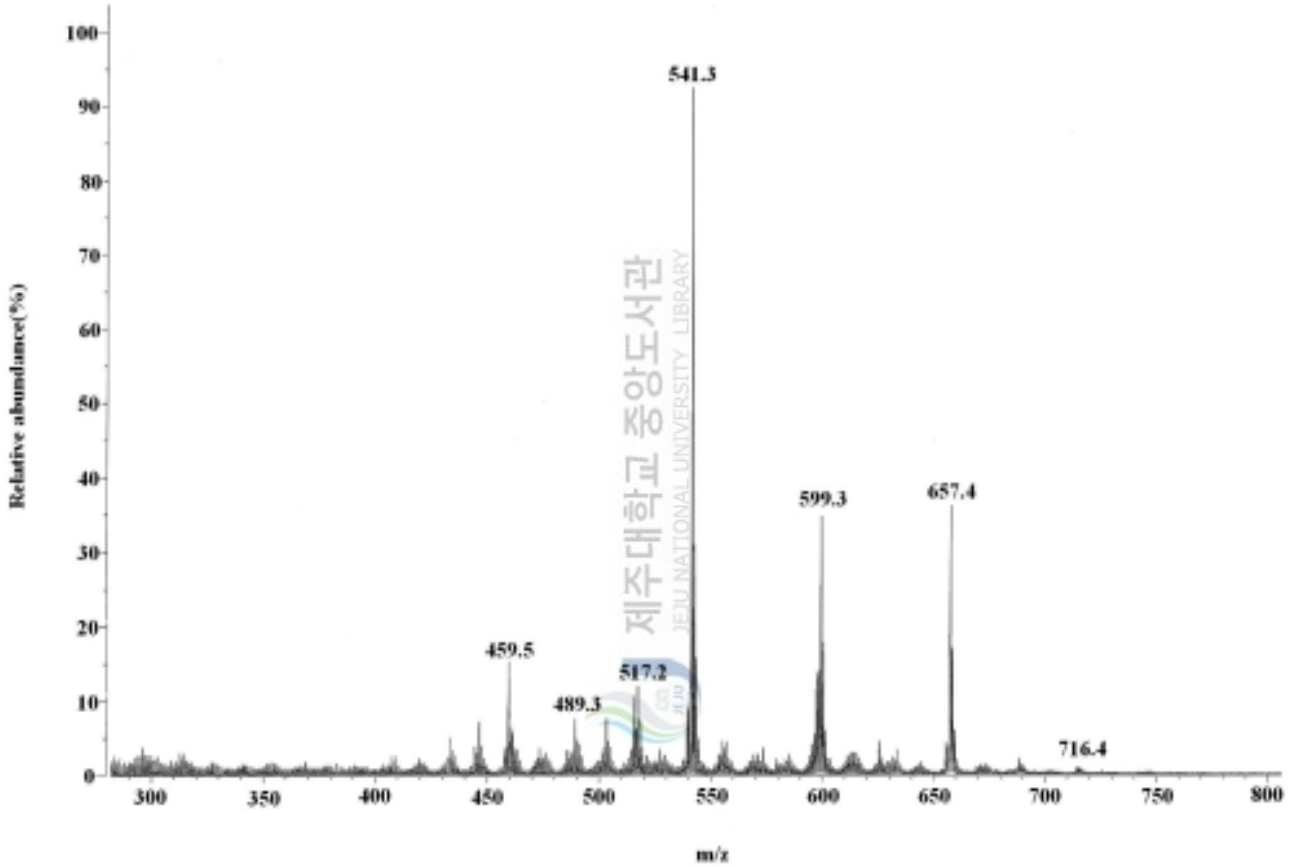

Figure. 16. FAB mass spectrum of the $[Co_2([20]\text{-}DCHDC)(NCS)_2] \cdot 2H_2O$.

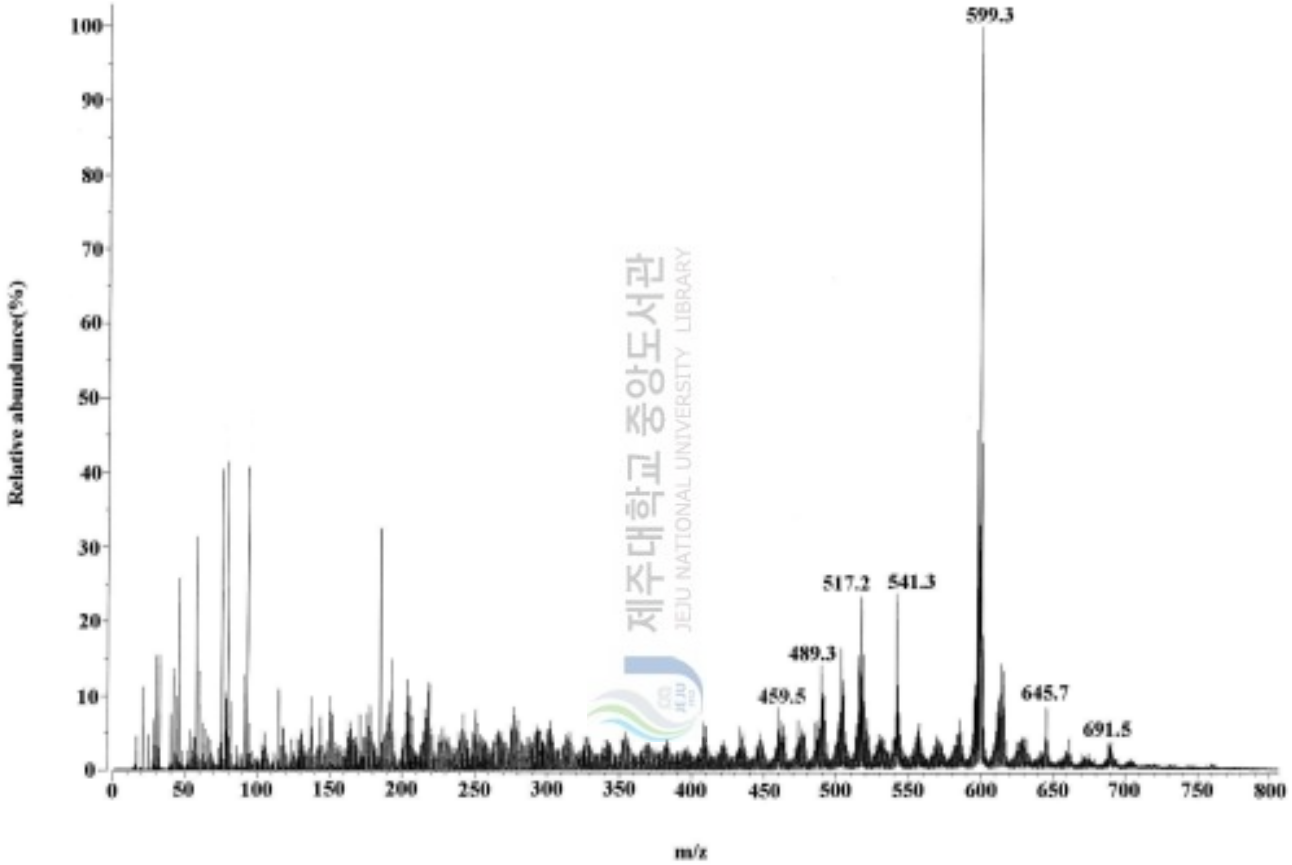

Figure. 17. FAB mass spectrum of the $[Co_2([20]\text{-}DCHDC)(NO_2)_2] \cdot 3.5H_2O$.

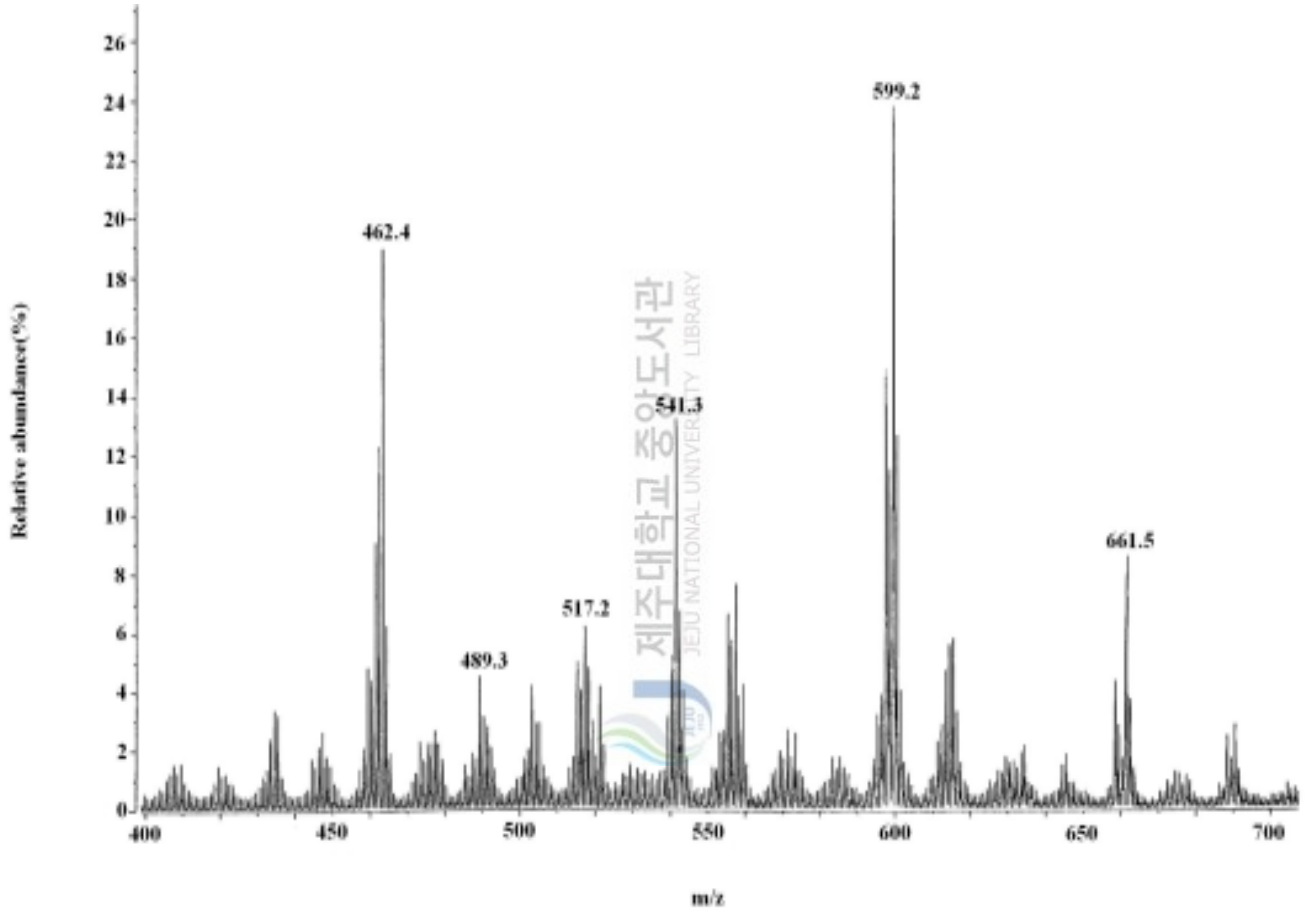

Figure. 18. FAB mass spectrum of the $[Co_2([20]\text{-}DCHDC)(OH_2)_4](NO_3)_2$.

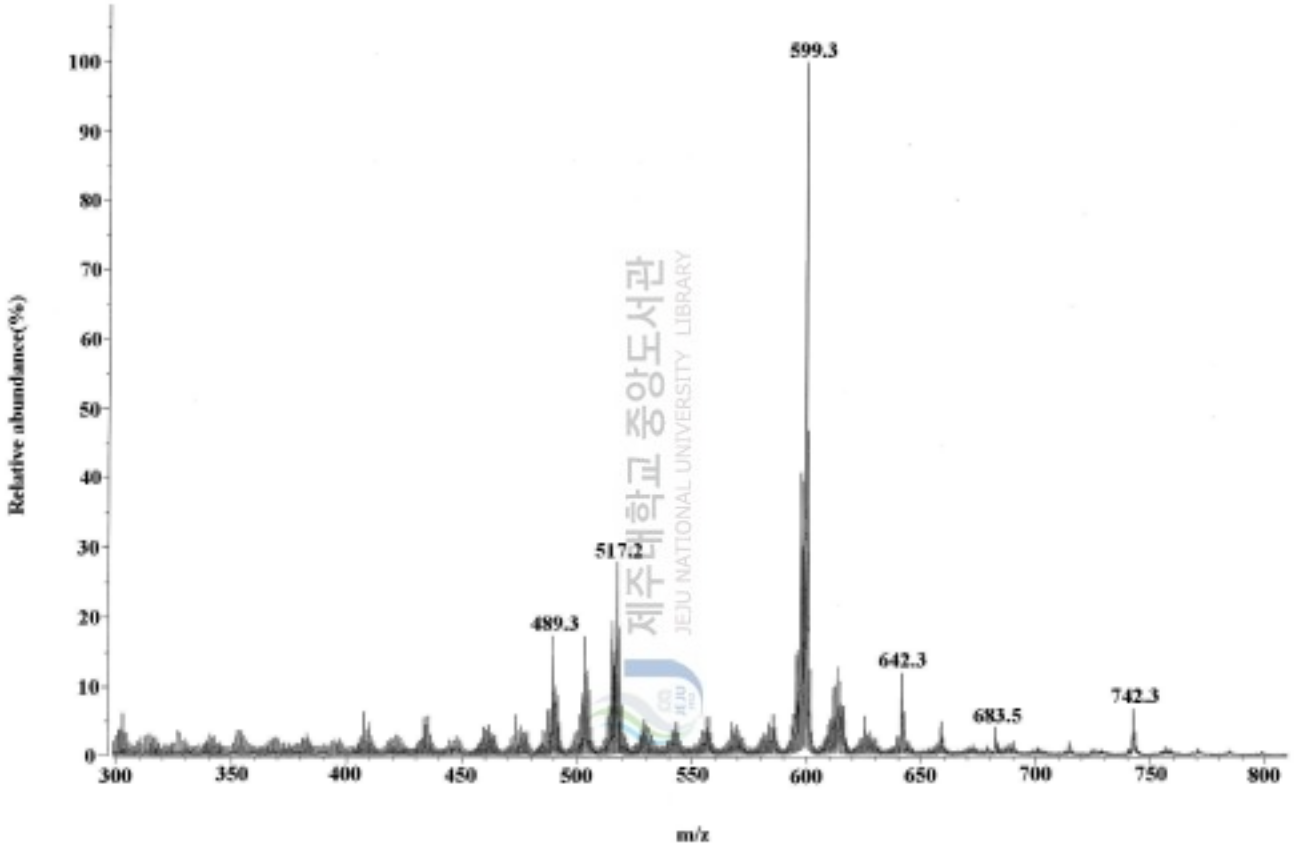

Figure. 19. FAB mass spectrum of the $[Co_2([20]\text{-DCHDC})(N_3)_3(OH)]$.

4. Electronic absorption spectra of the complexes

The electronic absorption spectra of Co(Ⅱ or Ⅲ) complexes at room temperature were represented in Figure. 20～26 and summarized Table 4. The dark green crystals of complex $[Co_2([20]\text{-}DCHDC)Cl_2] \cdot 2H_2O$ become dark brown in DMSO. The electronic absorption spectrum of this solution is typical of six- coordinate cobalt(II) complex indicating that species existing in solution is $[Co_2([20]\text{-}DCHDC)(H_2O)_4]^{2+}$. A shoulder band appears at around 600nm(ε = 36 - 129 $M^{-1}cm^{-1}$) due to metal *d-d* electronic transitopns. However, strong absorptions at 400 - 451 nm(ε = 458 - 1384 $M^{-1}cm^{-1}$) are clearly associated with ligand to metal charge transfer(LMCT) transitions. [39]

Table 4. Electronic spectra data for the Co(Ⅱor Ⅲ) complexes.

Complexes	medium	λ_{max}, nm (ε, M^{-1} cm^{-1})	
		LMCT	*d-d*
$[Co_2([20]\text{-DCHDC})Cl_2]\cdot 2H_2O$	DMSO	413(635)	506sh(36)
	solid	471	643
$[Co_2([20]\text{-DCHDC})(\mu\text{-}O_2ClO_2)_2]\cdot H_2O$	DMSO	409(1,123)	
	solid	426	600sh
$[Co_2([20]\text{-DCHDC})(CN)_2]\cdot 2H_2O$	DMSO	439(1,167)	
	solid	440	560sh
$[Co_2([20]\text{-DCHDC})(NCS)_2]\cdot 2H_2O$	DMSO	402(1,384)	
	solid	444	583
$[Co_2([20]\text{-DCHDC})(NO_2)_2]\cdot 3.5H_2O$	DMSO	417(1,218)	
	solid	430	556sh
$[Co_2([20]\text{-DCHDC})(OH_2)_4](NO_3)_2$	DMSO	400(952)	
	solid	446	652sh
$[Co_2([20]\text{-DCHDC})(N_3)_3(OH)]$	DMSO	451(458)	608(129)
	solid	447	638

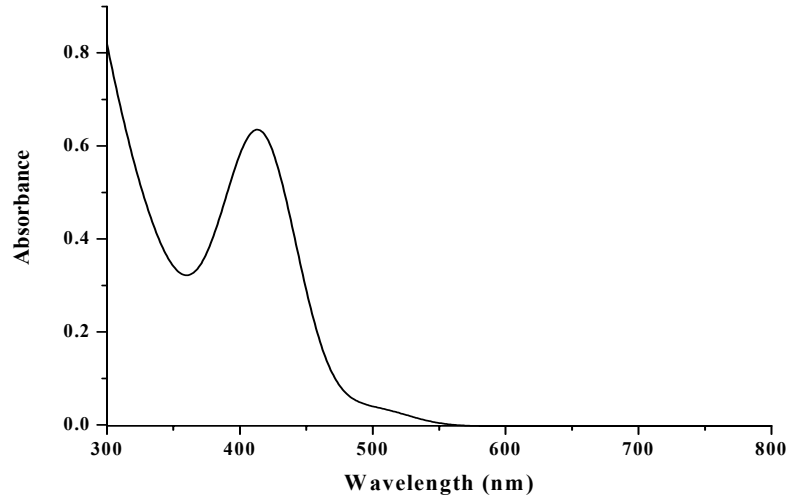

(a)

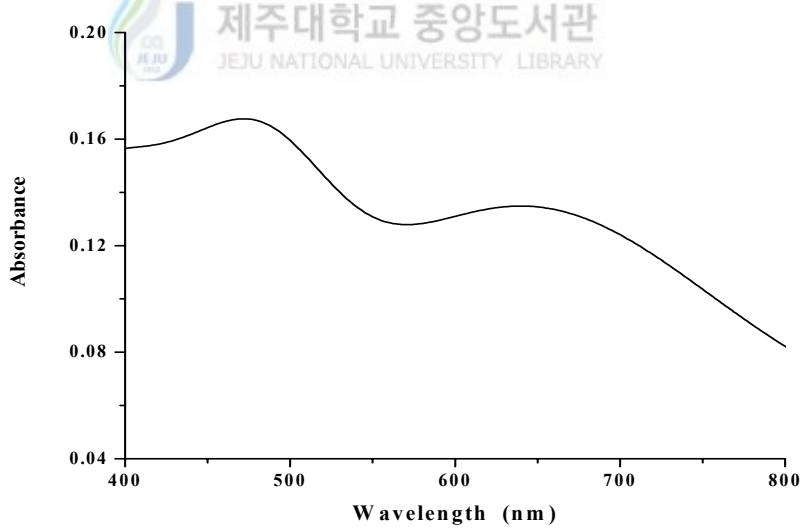

(b)

Figure. 20. Electronic absorption spectrum of $[Co_2([20]\text{-}DCHDC)Cl_2]\cdot 2H_2O$ in (a) DMSO (1.0×10^{-3}M) and (b) solid ($BaSO_4$).

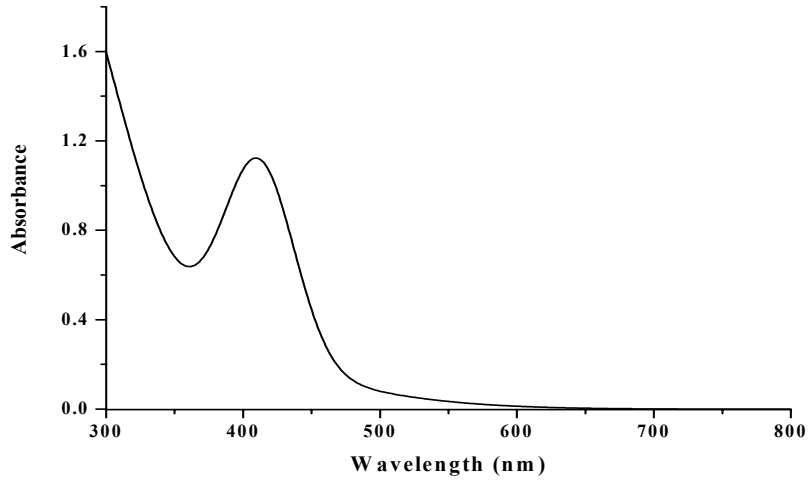

(a)

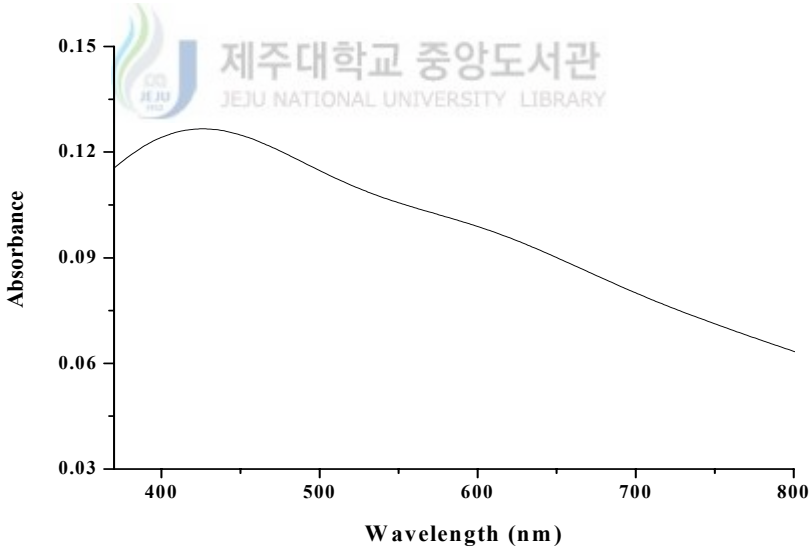

(b)

Figure. 21. Electronic absorption spectrum of $[Co_2([20]\text{-}DCHDC)(\mu\text{-}O_2ClO_2)_2]\cdot H_2O$ in (a) DMSO (1.0×10^{-3}M) and (b) solid ($BaSO_4$).

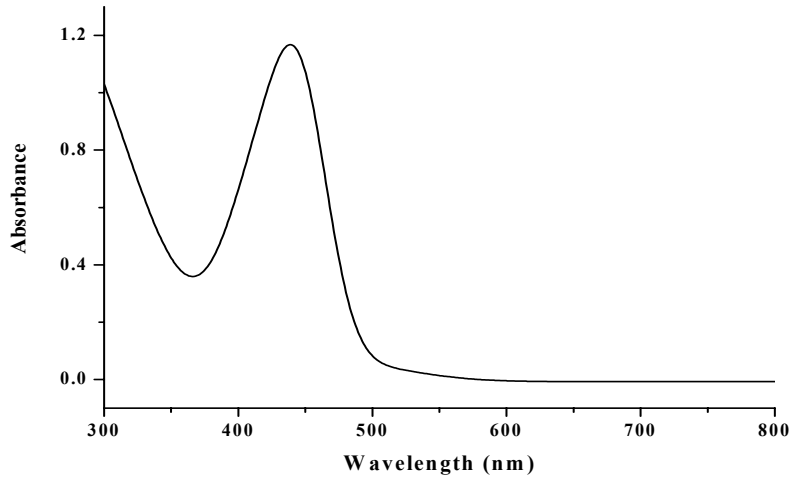

(a)

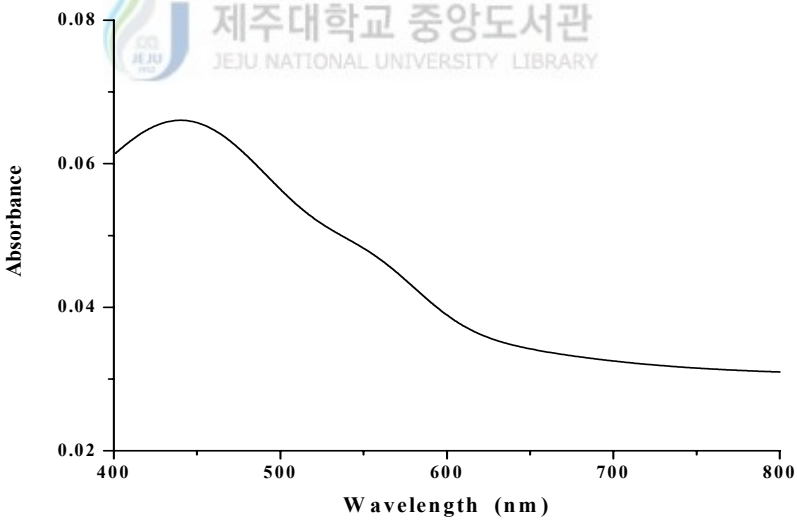

(b)

Figure. 22. Electronic absorption spectrum of $[Co_2([20]\text{-}DCHDC)(CN)_2]\cdot 2H_2O$ in (a) DMSO (1.0×10^{-3}M) and (b) solid ($BaSO_4$).

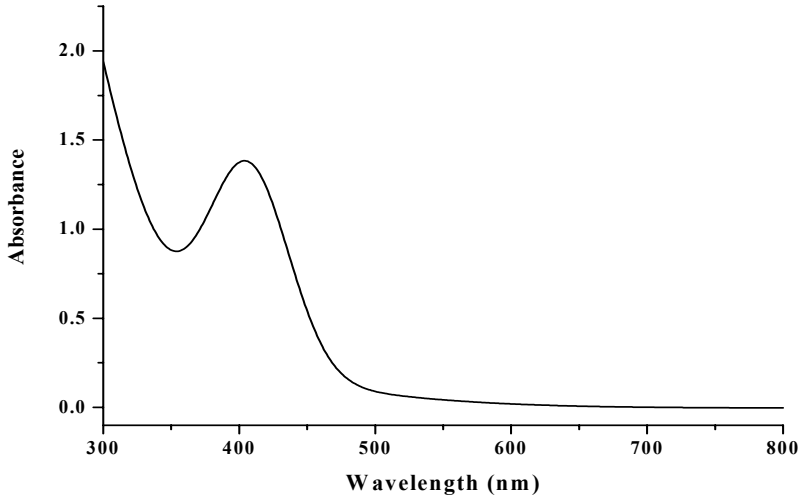

(a)

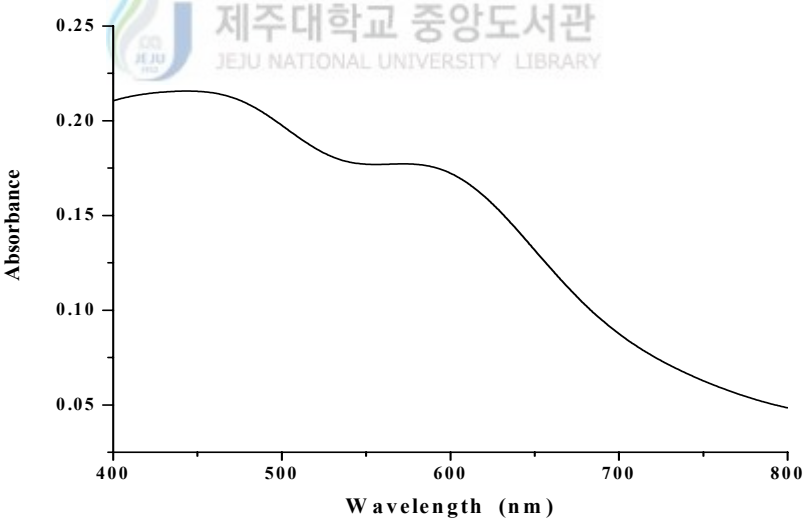

(b)

Figure. 23. Electronic absorption spectrum of $[Co_2([20]\text{-}DCHDC)(NCS)_2]\cdot 2H_2O$ in (a) DMSO (1.0×10^{-3}M) and (b) solid ($BaSO_4$).

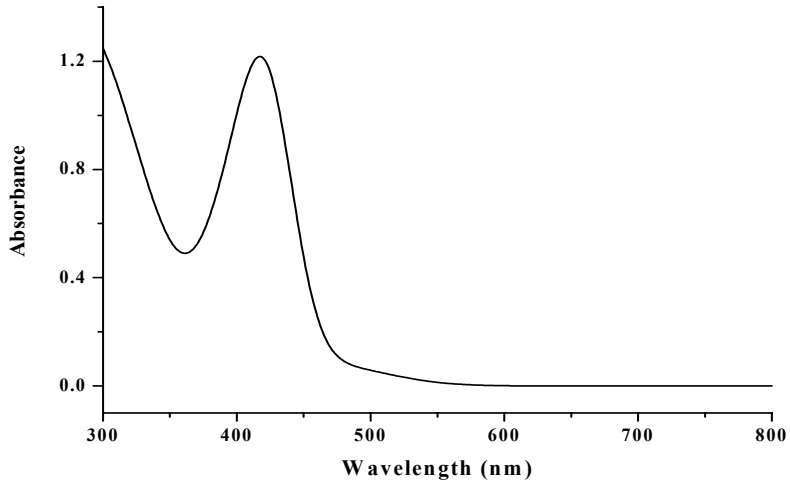

(a)

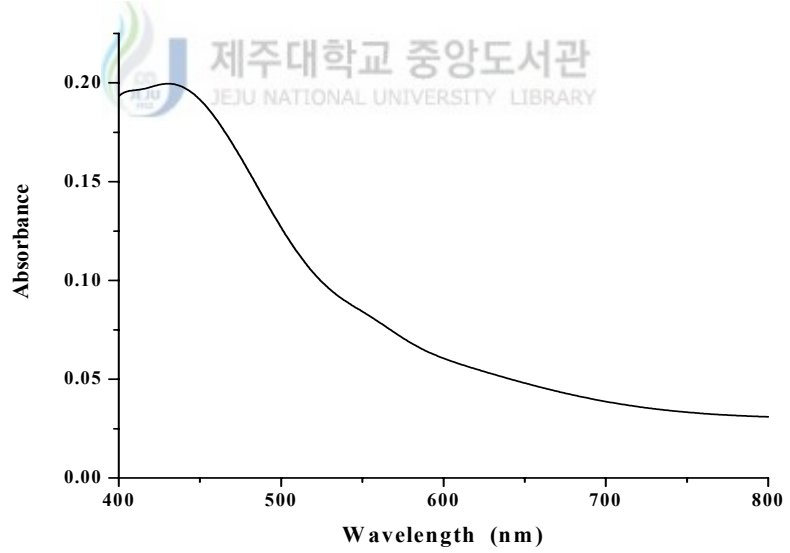

(b)

Figure. 24. Electronic absorption spectrum of $[Co_2([20]\text{-}DCHDC)(NO_2)_2]\cdot 3.5H_2O$ in (a) DMSO (1.0×10^{-3}M) and (b) solid ($BaSO_4$).

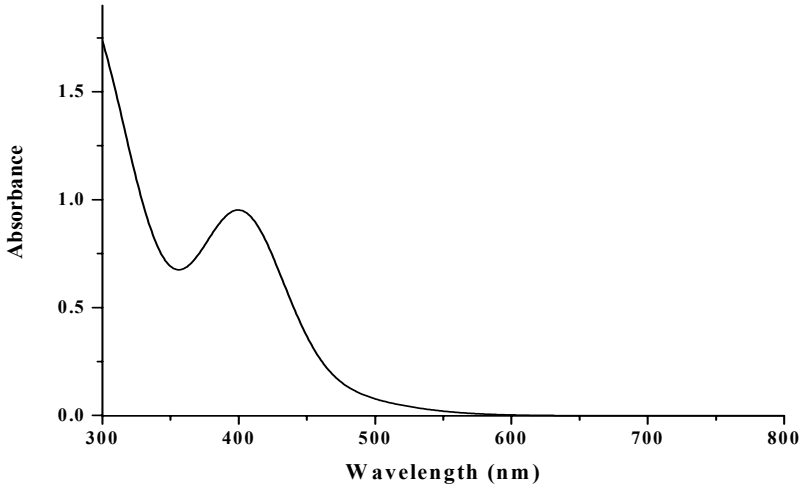

(a)

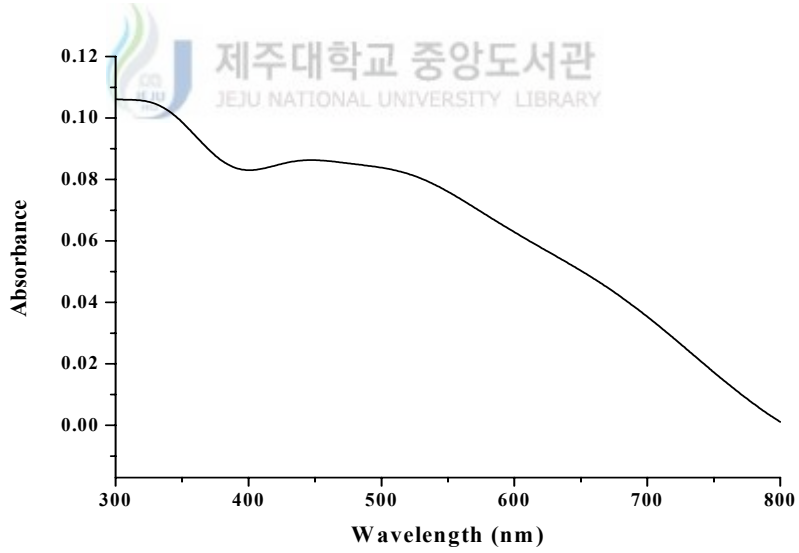

(b)

Figure. 25. Electronic absorption spectrum of $[Co_2([20]\text{-}DCHDC)(OH_2)_4](NO_3)_2$ in (a) DMSO (1.0×10^{-3}M) and (b) solid ($BaSO_4$).

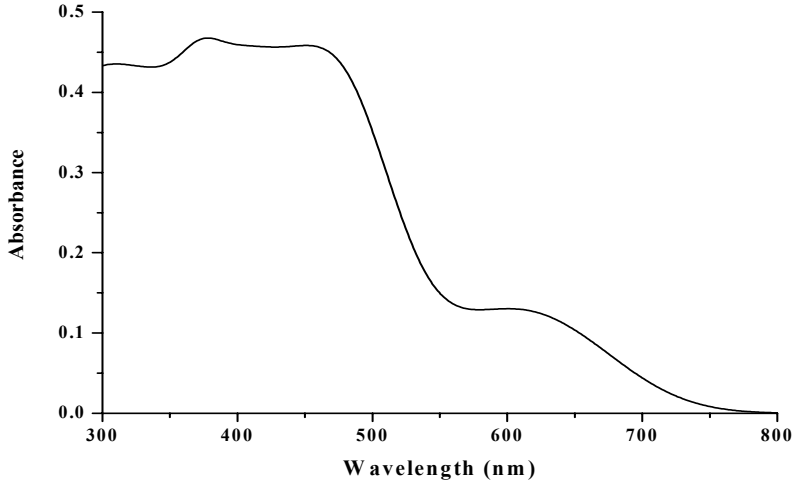

(a)

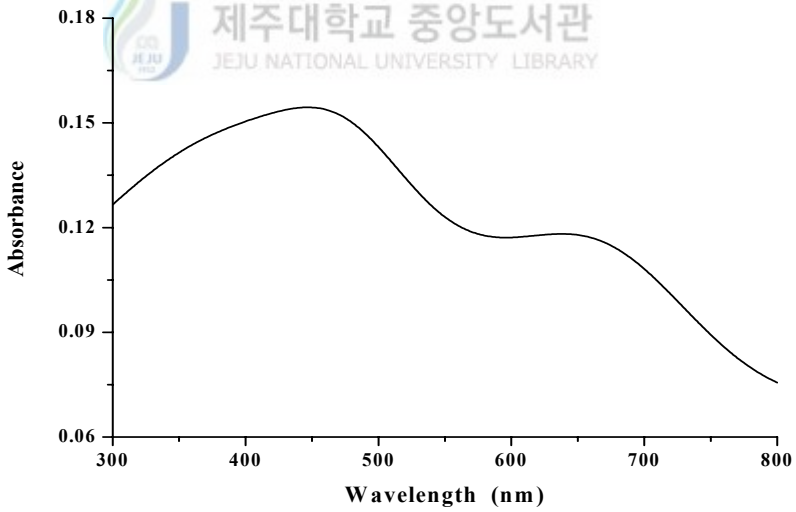

(b)

Figure. 26. Electronic absorption spectrum of $[Co_2([20]\text{-}DCHDC)(N_3)_3(OH)]$ in (a) DMSO (1.0×10^{-3}M) and (b) solid ($BaSO_4$).

IV. Conclusion

The reaction of 2,6-diformyl-*p*-cresol and trans-1,2-diaminocyclohexane in methanol in equimolar ratio using the high dilution technique affords a [3 + 3] Schiff-base macrocycle L_3 as yellow solid in high yield. The CHN, IR, NMR and FAB mass spectral data of the product do not agree with the expected a [2 + 2] Schiff-base macrocycle ligand L_2 (= H_2[20]-DCHDC) but match with the composition of [3 + 3] Schiff-base macrocycle L_3.

Dinuclear Co(Ⅱ or Ⅲ) complexe, $[Co_2([20]\text{-DCHDC})Cl_2]\cdot 2H_2O$, with [2 + 2] symmetrical N_4O_2 compartmental macrocyclic ligand containing bridging phenolic oxygen atoms was synthesized by metal template condensation of 2,6-diformyl-*p*-cresol, trans-1,2-diaminocyclohexane, and $CoCl_2 \cdot 6H_2O$. The reaction of $[Co_2([20]\text{-DCHDC})Cl_2]\cdot 2H_2O$ with auxiliary ligands (L_a ;ClO_4^-, CN^-, NCS^-, NO_2^-, NO_3^-, N_3^-) in aqueous solution formed a new 6 complexes; $[Co_2([20]\text{-DCHDC})(\mu\text{-}O_2ClO_2)_2] \cdot H_2O$, $[Co_2([20]\text{-DCHDC})(CN)_2] \cdot 2H_2O$, $[Co_2([20]\text{-DCHDC})(NCS)_2] \cdot 2H_2O$, $[Co_2([20]\text{-DCHDC})(NO_2)_2] \cdot 3.5H_2O$, $[Co_2([20]\text{-DCHDC})(OH_2)_4](NO_3)_2$, $[Co_2([20]\text{-DCHDC})(N_3)_3(OH)]$, where [20]-DCHDC is the dianion of the binucleating macrocyclic ligand 14,29-dimethyl-3,10,18,25-tetraazapentacyclo-[25,3,1,$0^{4,9}$,$1^{12,16}$,$0^{19,24}$]ditriacontane -2,10,12,14,16(32),17,27(31),28,30-decane-31,32-diol.

The strong and sharp absorption bands occurring at 1643～1632 cm^{-1} are attributed to ν(C=N) of the coordinated [(H_2[20]-DCHDC)] ligand, and the absence of any carbonyl bands associated with the diformylphenol starting materials or nonmarcrocyclic intermediates. A weak bands at near 461~459 cm^{-1} region associated with the Co-N(macrocycle) vibration.

The strong four bands at 1146, 1121, 1109, and 1089 cm^{-1} in $[Co_2([20]\text{-}DCHDC)(\mu\text{-}O_2ClO_2)_2] \cdot H_2O$ complex are attributed to a bridging bidentate ligand Co-O-ClO_2-O-Co. The absorption peak at 2125 cm^{-1} in the $[Co_2([20]\text{-}DCHDC)(CN)_2] \cdot 2H_2O$ is assigned to the stretching frequency of CN. Cyano complexes exhibit bands due to M-C stretching in the region 600-350 cm^{-1}, due to M-CN deformation in the region 130-60 cm^{-1}. The absorption vibrations due to the N-coordinated bonded NCS^- in $[Co_2([20]\text{-}DCHDC)(NCS)_2] \cdot 2H_2O$ appear 2071 and 837 cm^{-1}. The very strong absorption peaks at 1452 and 1312 cm^{-1} in the $[Co_2([20]\text{-}DCHDC)(NO_2)_2] \cdot 3.5H_2O$ are assigned to the antisymmetric and symmetric stretching mode of N-bonded NO_2, respectively. And deformation band of N-bonded NO_2 is observed at 654 cm^{-1}.

The absorption bands of coordinate nitrate occurring in the IR spectra of $[Co_2([20]\text{-}DCHDC)(OH_2)_4](NO_3)_2$ in the 1454, 1313 and 1038 cm^{-1} regions are assignable to the ν(N=O) (ν_1), $\nu_a(NO_2)$ (ν_5) and $\nu_s(NO_2)$ (ν_2) vibrations, respectively. The very strong absorption band at 1385 cm^{-1} is characteristic of ionic nitrate present in the outer-coordination sphere. The absorption peaks at 2034 and 2010 cm^{-1} in the $[Co_2([20]\text{-}DCHDC)(N_3)_3(OH)]$ are assigned to the asymmetric stretching mode of coordinated azide. The symmetric stretching frequency of coordinated azide is observed at 1286 cm^{-1}. And deformation band of coordinated azide is observed at 652 cm^{-1}.

The molecular ion loses the exocyclic ligands resulting in the formation of the fragment $[Co_2([20]\text{-}DCHDC)]^+$. All these species are well observed in the FAB mass spectra at m/z 599. α-cleavage peaks of one cyclohexane from the $[Co_2([20]\text{-}DCHDC)]^+$ ion in the formation of the fragment $[Co_2(L_{ac})]^+$ are observed at m/z 518 region. Removal peaks of one cobalt ion from the

$[Co_2([20]\text{-DCHDC})]^+$ ion in the formation of the fragment $[Co([20]\text{-DCHDC})]^+$ is observed at m/z 541. α-cleavage peaks of one cyclohexane from the $[Co([20]\text{-DCHDC})]^+$ ion in the formation of the fragment $[Co(L_{ac})]^+$ are observed at m/z 461 region. The FAB mass spectra of all the complexes contain peaks corresponding to the $[(H_2[20]\text{-DCHDC})]^+$ fragment ion at m/z 489 region. This indicates that the species $[Co_2([20]\text{-DCHDC})]^+$ undergoes demetallation to give the tetraazadioxa macrocycle $H_2[20]$-DCHDC under FAB conditions. These peaks are associated with peaks of mass one or two greater or less, which are attributed to protonated /deprotonated forms. This also accounts for the slight ambiguities in making assignments.

The week molecular ion peaks corresponding to the $[Co_2([20]\text{-DCHDC})(ClO_4)]^+$, $[Co_2([20]\text{-DCHDC})(CN)_2]^+$, $[Co_2([20]\text{-DCHDC})(NCS)_2]^+$, $[Co_2([20]\text{-DCHDC})(NO_2)_2]^+$, $[Co_2([20]\text{-DCHDC})(NO_3)]^+$, and $[Co_2([20]\text{-DCHDC})(N_3)_3(OH)]^+$ are observed at m/z 699.1, 652.1, 716.1, 692.1, 662.1 and 743.2, respectively.

The electronic absorption spectrum of this solution is typical of six-coordinate cobalt(II) complex indicating that species existing in solution is $[Co_2([20]\text{-DCHDC})(H_2O)_4]^{2+}$. A shoulder band appears at around 600nm(ε = 36 - 129 $M^{-1}cm^{-1}$) due to metal *d-d* electronic transitions. However, strong absorptions at 400 - 451 nm(ε = 458 - 1384 $M^{-1}cm^{-1}$) are clearly associated with ligand to metal charge transfer(LMCT) transitions.

References

[1] B. Dietrich, P. Viout, and J. -M. Lehn, *Macrocyclic Chemistry*, VCH Verlagsgesellschaft, Weinheim, **1993**.

[2] J. -M. Lehn, *Supramolecular Chemistry*, VCH Verlagsgesellschaft, Weinheim, **1995**.

[3] E. C. Constable, *Metals and Ligand Reactivity*, VCH Verlagsgesellschaft, Weinheim, **1996**.

[4] J. R. Fredericks and A. D. Hamilton, in: A. D. Hamilton (Ed.), *Supramolecular Control of Structure and Reactivity*, Wiley, Chichester, **1996**, Chapter 1.

[5] J. W. Steed and J. L. Atwood, *Supramolecular Chemistry*, Wiley, Chichester, **2000**.

[6] D. Kong, J. Mao, Arthur E. Martell , A. Clearfield *Inorg. Chim. Acta* 335 (**2002**) 7

[7] M. J. Heeg and S. S. Jurisson, *Acc. Chem. Res.* 32 (**1999**), 1053.

[8] (a) D. E. Fenton and P. A. Vigato, *Chem. Soc. Rev.* 17 (**1988**), 69; (b) S. R. Collinson and D. E. Fenton, *Coord. Chem. Rev.* 148 (**1996**), 19; (c) H. Ōkawa, H. Furutachi, and D. E. Fenton, *Coord. Chem. Rev.* 174 (**1998**), 51.

[9] L. M. J. Vallarino, in: K. A. Gschneidner Jr. and L. Eyring (Eds.), *Handbook on the Physics and Chemistry of Rare Earths*, vol. 15, Elsevier, Amsterdam, **1991**, Chapter 104.

[10] V. Alexander, *Chem. Rev.* 95 (**1995**), 273.

[11] R. Hernández-Molina and A. Mederos, in: J. A. McCleverty and T. J. Meyer (Eds.), *Comprehensive Coordination Chemistry II*, vol. 1, Elsevier, **2004**, Chapter 19.

[12] N. F. Curtis, in: J. A. McCleverty and T. J. Meyer (Eds.), *Comprehensive Coordination Chemistry II*, vol. 1, Elsevier, **2004**, Chapter 20.

[13] (a) S. Brooker, *Coord. Chem. Rev.* 222 (**2001**), 33; (b) S. Brooker, *Eur. J. Inorg. Chem.* (**2002**), 2535.

[14] (a) D. H. Bush, A. L. Vance and A. G. Kolochinksii, in: J. -M. Lehn (Ed.), *Comprehensive Supramolecular Chemistry*, vol. 9, Pergamon Press, **1996**, Chapter 1; (b) N. V. Gerbeleu, V. B. Arion and J. Burges, *Template Synthesis of Macrocyclic Compounds*, Wiley-VCH, Weinheim, **1999**.

[15] S. M. Nelson, C. V. Knox, M. McCann, and M. G. B. Drew, J. *Chem. Soc., Dalton Trans.* (**1981**), 1659.

[16] W. Radecka-Paryzek, *Inorg. Chim. Acta* 35 (**1979**), 349.

[17] W. Radecka-Paryzek, M. Kaczmarek, V. Patroniak, and I. Pospieszna -Markiewicz, *J. Alloys Compd.* 323-324 (**2001**) 173.

[18] V. Patroniak and W. Radecka-Paryzek, *Mater. Sci. Eng. C* 18 (**2001**), 113.

[19] W. Radecka-Paryzek, M. Kaczmarek, I. Pospieszna-Markiewicz, *Pol. J. Chem.* 76 (**2002**), 679.

[20] W. Radecka-Paryzek, M. Kaczmarek, V. Patroniak, and I. Pospieszna -Markiewicz, *Inorg. Chem. Commun.* 6 (**2003**), 26.

[21] M. Kaczmarek, I. Pospieszna-Markiewicz, and W. Radecka-Paryzek, *J. Inclusion Phenom. Macrocyclic Chem.* 49 (**2004**) 115.

[22] I. Pospieszna-Markiewicz and W. Radecka-Paryzek, *J. Alloys Compd.* 374 (**2004**), 254.

[23] S. Kobayashi, T. Hamada, S. Nagayama, and K. Manabe, *Org. Lett.* 3 (**2001**), 165.

[24] T. Hamada, K. Manabe, S. Ishikawa, S. Nagayama, M. Shiro, and S. Kobayashi, *J. Am. Chem. Soc.* 125 (**2003**), 2989.

[25] S. W. A. Bligh, N. Choi, W. J. Cummins, E. G. Evagorou, J. D. Kelly, and M. McPartlin, *J. Chem. Soc., Dalton Trans.* (**1994**), 3369.

[26] J. Lisowski and P. Starynowicz*, Polyhedron* 19 (**2000**) 465-469.

T. Tsubomura, K. Yasaku, T. Sato, and M. Morita, *Inorg. Chem.* 31 (**1992**), 447.

[27] D. D. Perrin and W. L. F. Armarego, *Purification of Laboratory Chemicals, Pergamon,* 3rd edn., **1988**.

[28] T. Shozo, *Bull. Chem. Soc. Jpn*. 57 (**1984**), 2683.

[29] J. C. Byun, Y. C. Park, and C. H. Han, *J. Kor. Chem. Soc.* 43/3 (**1999**), 267.

[30] S. R. Korupoju, N. Mangyakarasi, S. Ameerunisha. and P. S. Zacharias, *J. Chem. Soc.,Dalton Trans.,* (**2000**), 2845..

[31] L. A. Kahwa, J. Selbin, T. C. Y. Hsieh and R. A. Laine, *Inorg. Chim. Acta* 118 (**1986**), 179.

[32] D. Suresh Kumar and V. Alexander, *Inorg. Chim. Acta* 238(**1995**), 63.

[33] G. Socrates, *Infrared and Raman Charateristic Group Frequencies*. 3rd edn., Wiley, New York, **2001**, p. 299.

[34] G. Socrates, *Infrared and Raman Charateristic Group Frequencies*. 3rd edn., Wiley, New York, **2001**, p. 309.

[35] G. Socrates, *Infrared and Raman Charateristic Group Frequencies*. 3rd edn., Wiley, New York, **2001**, p. 320.

[36] G. Socrates, *Infrared and Raman Charateristic Group Frequencies*. 3rd edn., Wiley, New York, **2001**, p. 321.

[37] G. Socrates, *Infrared and Raman Charateristic Group Frequencies*. 3rd edn., Wiley, New York, **2001**, p. 317.

[38] P. Guerriero, U. Casellato, S. Tamburini, P. A. Vigato and R. Graziani, *Inorg. Chim. Acta* 129 (**1987**), 127.

[39] D. Sutton, *Electronic Spectra of Transition Metal Complexes*, McGraw -Hill, London, **1968**.

2,6-diformyl-*p*-cresol과 *trans*-1,2-diaminocyclohexane에 의한 N_4O_2 칸막이형 거대고리-cobalt(Ⅱ or Ⅲ) 착물과 보조 리간드간의 화합물 합성 및 특성

현 창 식

제주대학교 교육대학원 화학 교육전공

지도교수: 변 종 철

2,6-diformyl-*p*-cresol과 *trans*-1,2-diaminocyclohexane을 고리축합 반응은 [2+2] 거대고리 리간드(L_2)로 형성되지 않고, [3+3]형태의 Schiff base 거대고리 리간드(L_3)가 형성되었다. 반면, 2,6-diformyl-*p*-cresol과 *trans*-1,2-diaminocyclohexane에 $CoCl{\cdot}6H_2O$를 금속주형 축합반응을 시켰을 경우에는 페놀의 산소원자가 다리 결합을 하고 있는 이핵 Co(II)의 20-원 N_4O_2 칸막이형 거대고리 착물 $[Co_2([20]\text{-DCHDC})Cl_2]{\cdot}2H_2O$ (H_2[20]-DCHDC; 14,29-dimethyl-3,10,18,25-tetraazapentacyclo-[25,3,1,$0^{4,9}$,$1^{12,16}$,$0^{19,24}$]ditriacontane-2,10,12,14,16(32),17,27(31),28,30-decane-31,32-diol)을 합성하였다. $[Co_2([20]\text{-DCHDC})Cl_2]{\cdot}2H_2O$을 수용액 하에서 보조리간드 ($L_a$; ClO_4^-, CN^-, SCN^-, NO_2^-, NO_3^-, N_3^-)와 반응시켜 새로운 Co(Ⅱ or Ⅲ) 이핵 착물 6개, $[Co_2([20]\text{-DCHDC})(\mu\text{-}O_2ClO_2)_2]\cdot H_2O$, $[Co_2([20]\text{-DCHDC})(CN)_2]\cdot 2H_2O$, $[Co_2([20]\text{-DCHDC})(NCS)_2]\cdot 2H_2O$, $[Co_2([20]\text{-DCHDC})(NO_2)_2]\cdot 3.5H_2O$, $[Co_2([20]\text{-DCHDC})(OH_2)_4](NO_3)_2$, $[Co_2([20]\text{-DCHDC})(N_3)_3(OH)]$를 합성하였다. 이 착물 들은 원소분석, 전기전도도, UV/Vis, IR 분광법 및 질량 분석법 등을 이용하여 특성 및 구조적 성질을 확인·고찰하였다.

※본 論文은 2005년 8월 濟州大學校 敎育大學院 委員會에 提出된 敎育學 碩士學位 論文임.